



Research Report

Spatiotemporal patterns of sensorimotor fMRI activity influence hand motor recovery in subacute stroke: A longitudinal task-related fMRI study



Fabrice F. Hannanu ^a, Issa Goundous ^a, Olivier Detante ^b,
Bernadette Naegel ^b and Assia Jaillard ^{a,c,d,*}

^a AGEIS, EA 7407, Université Grenoble Alpes, Grenoble, France

^b Stroke Unit, Neurologie, Centre Hospitalier Universitaire Grenoble Alpes (CHUGA), Grenoble, France

^c Unité IRM 3T Recherche - IRMaGe, Inserm US 17 CNRS - UMS 3552 UGA, CHUGA, Grenoble, France

^d Pôle Recherche, CHUGA, Grenoble, France

ARTICLE INFO

Article history:

Received 9 July 2019

Revised 27 November 2019

Accepted 13 March 2020

Published online 17 April 2020

Keywords:

Dexterity

Stroke

fMRI

Recovery

Primary motor cortex

ABSTRACT

Motor hand deficits impact autonomy in everyday life, and neuroplasticity processes of motor recovery can be explored using functional MRI (fMRI). However, few studies have used fMRI to explore the mechanisms underlying hand recovery following stroke. Based on the dual visuomotor model positing that two segregated dorsomedial and dorsolateral cerebral networks control reach and grasp movements, we explored the relationship between motor task-related activity in the sensorimotor network and hand recovery following stroke.

Behavioral recovery was explored with a handgrip force task assessing simple grasp, and a visuomotor reaching and precise grasping task, the Purdue Pegboard Test (PPT). We used a passive wrist flexion-extension task to measure fMRI activity in 36 sensorimotor brain areas. Behavioral and fMRI measurements were performed in 27 patients (53.2 ± 9.5 years) 1-month following stroke, and then 6-month and 24-month later. The effects of sensorimotor activity on hand recovery were analyzed using correlations and linear mixed models (LMMs).

PPT and handgrip force correlated with fMRI activity measures in the sensorimotor and parietal areas. PPT recovery was modeled by fMRI measures in the ipsilesional primary motor cortex (MI-4p), superior parietal lobule (SPL-7M) and parietal operculum OP1, and lesion side. Handgrip force was modeled by ipsilesional MI-4a, OP1, and contralesional inferior parietal lobule (IPL-PFt). Moreover, the relationship between fMRI activity and hand recovery was time-dependent, occurring in the early recovery period in SPL-BA-7M, and later in MI.

These results suggest that areas of both dorsolateral and dorsomedial networks participate to visuomotor reach and grasp tasks (PPT), while dorsolateral network areas may control recovery of simple grasp (handgrip force), suggesting that the type of movement modulates network recruitment. We also found functional dissociations between MI-

* Corresponding author. Unité IRM 3T - Recherche CHU Grenoble Alpes, CS 10217 38043 Grenoble Cedex 9, France.

E-mail address: Assia.Jaillard@univ-grenoble-alpes.fr (A. Jaillard).

<https://doi.org/10.1016/j.cortex.2020.03.024>

0010-9452/© 2020 Elsevier Ltd. All rights reserved.

4p related to PPT that required independent finger movements and MI-4a related to simple grasp without independent finger movements. These findings need to be replicated in further studies.

© 2020 Elsevier Ltd. All rights reserved.

1. Introduction

Stroke remains a leading cause of acquired motor disability in adults, with manual dexterity being often impaired following stroke (Horn, Grothe, & Lotze, 2016). As new therapies are emerging in stroke, approaches to identify mechanisms and biomarkers of motor recovery of the paretic hand using MRI are needed. Furthermore, prognostic measures to assess the individual potential for improvement are also an important step in developing more targeted interventions. To this end, functional neuroimaging techniques may provide an insight into neuroplasticity processes involved in motor recovery to develop tailored programs of rehabilitation following stroke (Horn et al., 2016). Among the currently available MRI techniques, functional MRI (fMRI) using motor task paradigms is considered as a potential tool in stroke recovery studies because of its ability to allow dynamic representation of motor activity. Typical patterns related to hand motor tasks in healthy participants are characterized by increased activity in the canonical sensorimotor areas, comprising the contralateral premotor cortex (PMC), primary sensorimotor cortex (SI, MI), Supplementary Motor Area (SMA), and ipsilateral cerebellum (anterior cerebellum or IV, V, VI lobules and posterior cerebellum or VIII lobules) (Keisker, Hepp-Reymond, Blickenstorfer, Meyer, & Kollias, 2009). Of note, both passive and active motor tasks activate the sensorimotor cortex (Berlot, Prichard, O'Reilly, Ejaz, & Diedrichsen, 2019; Blatow et al., 2011; Weiller et al., 1996), as well as the other areas of the sensorimotor network such as the posterior parietal regions (Estevez et al., 2014; Loubinoux et al., 2001). In stroke, fMRI activity related to movements of the paretic hand has been observed in both ipsilesional and contralesional frontoparietal regions (Lotze et al., 2012; Marshall et al., 2000; Rehme et al., 2015). Typically, the restoration of a normal motor pattern is typically associated with good motor outcomes (Favre et al., 2014; Rehme, Eickhoff, Rottschy, Fink, & Grefkes, 2012). Furthermore, there is increasing evidence that measures of motor related fMRI activity in the sensorimotor network correlate with motor performance assessed outside the scanner (Hannanu et al., 2017; Loubinoux et al., 2003; Rehme et al., 2012), and can predict motor recovery (Favre et al., 2014; Hannanu et al., 2017; Loubinoux et al., 2007; Rehme et al., 2015; Richards, Stewart, Woodbury, Senesac, & Cauraugh, 2008).

Prehension is a basic and pivotal component of daily-life functional tasks for the manipulation of objects (Frey, 2008). Manual prehension consists of two temporally integrated movements, reach and grasp, each mediated by different neural pathways from the visual to motor cortex (Goodale & Milner, 1992; Jeannerod, Arbib, Rizzolatti, & Sakata, 1995;

Pandya, 2015a). First, Milner (Milner & Goodale, 2008) and Goodale (Goodale & Milner, 1992) proposed the coexistence of a ventral circuit for object identification, and a dorsal circuit from the visual cortex via the posterior parietal to premotor and motor regions for visually guided actions directed at objects. A more recent view (Culham & Valyear, 2006) based on the macaque model (Borra, Gerbella, Rozzi, & Luppino, 2017) and neuroimaging studies in humans (Cavina-Pratesi et al., 2010) posits that two specialized dorso-parietofrontal circuits control prehension, both of which include projections to MI. In humans, the dorsolateral circuit connects the anterior bank of the intraparietal sulcus (aIPS) and inferior parietal lobule (IPL) to the ventral premotor cortex (PMv) for generating purposeful hand actions such as grasping, including hand pre-shaping as well as some programming aspects of grasping and manipulation of objects that require precision (Culham & Valyear, 2006; Davare, Andres, Clerget, Thonnard, & Olivier, 2007).

The dorsomedial circuit connects the superior parieto-occipital cortex (SPOC) and superior parietal lobule (SPL = BA5 and BA7) to the dorsolateral premotor cortex (PMd = dorsolateral BA6), where visuospatial processing can combine appropriate sensorimotor information to monitor the different phases of reaching (Cavina-Pratesi et al., 2010; Filimon, Nelson, Hagler, & Sereno, 2007; Filimon, Nelson, Huang, & Sereno, 2009; Vesia et al., 2017). However this dual visuomotor circuit model has been challenged with recent evidence of a more complex arrangement in both human (Grol et al., 2007) and nonhuman primates (Nelissen, Fiave, & Vanduffel, 2018). First, functional neuroimaging and TMS studies have shown that grasping tasks may involve both dorsomedial and dorsolateral circuits, although with different timings, according to the type and the degree of precision required by the movement (Davare, Andres, Cosnard, Thonnard, & Olivier, 2006; Grol et al., 2007). Second, fMRI studies have revealed that PMd and SMA were activated for grasp movements without reach component (Cavina-Pratesi et al., 2010). Third, TMS (Vesia et al., 2017) and fMRI (Cavina-Pratesi et al., 2010) studies have shown that the anterior SPOC, which includes the putative human homologue of V6A (Pitzalis, Fattori, & Galletti, 2015) and belongs to the dorso-medial circuit, controls grip components that might be integrated in goal directed actions. These findings are in line with nonhuman primate works showing that the dorsomedial reaching circuit, and more specifically V6Ad, conveyed aspects of grasp-specific information (Nelissen et al., 2018).

Along these lines (Budisavljevic et al., 2017), have correlated diffusion tractography with kinematic data in 30 healthy participants to explore the selectivity of fronto-parietal connections of the three branches of superior longitudinal

fasciculus (SLF, including SLFI, SLFII and SLFIII) for different components of a hand reach and grasp paradigm. The authors found that bilateral SLFII and SLF III were associated with the kinematic markers of both reaching and grasping components of action (Budisavljevic et al., 2017), suggesting that a common network supports visuomotor processing to generate and control reaching and reach and grasp movements (Budisavljevic et al., 2017; Howells et al., 2018).

Nevertheless, there is some agreement in the literature that reach and grasp movements are to some extent subserved by segregated visuomotor frontoparietal pathways, with a dissociation between the dorsomedial/reach circuit and the dorsolateral/grasp circuit (Cavina-Pratesi et al., 2018; Grafton, 2010; Karl & Whishaw, 2013; Vesia et al., 2017). The human dorsolateral/grasp circuit, similarly to the grasping lateral network in the macaque (Borra et al., 2017), comprises SMI, PMd and PMv, SMA, aIPS, SII (human OP1 and OP4), thalamus, and cerebellum (Cavina-Pratesi et al., 2018; Ehrsson et al., 2000). Moreover, while there are multiple actions that can be combined to generate grasp behaviors, two main components, grip force and precision grasping, have emerged (Ehrsson et al., 2000; Grafton, 2010). The pattern of activity for grip tasks in which fingers need to generate an appropriate grip force includes the IPL, pallidum, anterior insula, and cingulate motor area (CMA) in addition to the common grasp-related pattern (Cramer et al., 2002; Dettmers et al., 1995; Keisker et al., 2009). Moreover, the degree of force exerted was directly proportional to the amplitude of the brain signal determined by fMRI in the sensorimotor cortex and the anterior cerebellum (Keisker et al., 2009). A relationship between force and fMRI signal was also observed for PMv and IPL (Dai, Liu, Sahgal, Brown, & Yue, 2001; Keisker et al., 2009), with more controversial findings for SMA and CMA (Dai et al., 2001; Dettmers et al., 1995; Keisker et al., 2009). This suggests that network activity in areas of the dorsolateral circuit (MI, PMv, IPL) is necessary for controlling static force of finger muscles (Dai et al., 2001). For precision grasp, such as the grasp used in reach to grasp tasks, the key hubs include the aIPS and PMv in the dorsolateral network, and V6A, PMd, and SMA in the dorsomedial network (Cavina-Pratesi et al., 2010, 2018; Culham & Valyear, 2006; Vesia et al., 2017).

Taken together, these studies suggest that dorsolateral and dorsomedial circuits interact to achieve appropriate grasping behaviors, arguing against the dual visuomotor model viewing two independent fronto-parietal pathways to be responsible for reaching (dorsomedial network) and grasp movements (dorsolateral network). As previously suggested by (Grafton, 2010; Milner & Goodale, 2008), one approach to address some of the issues raised in the literature would be to account for the type of the task, as many paradigms engage some degree of both reach and grasp components. Accordingly, we hypothesized that a prototypical grasping task (without reach movement) would be subserved by the dorsolateral circuit, while tasks combining reach and fine grasp movements would engage both circuits.

We were also interested to explore the visuomotor model in the primary motor cortex (MI), which is the common output of the dorsolateral and dorsomedial circuits (Karl & Whishaw, 2013). In both human (Geyer et al., 1996) and nonhuman primates (He, Dum, & Strick, 1993), MI area can be divided into

two subregions. In the human brain, MI-4a and MI-4p differ in terms of cyto-, myelo- and chemoarchitectony: MI-4a is lying in the rostral part of MI located caudally to the dorsal premotor cortex, and MI-4p is the caudal part lying in the depth of the central sulcus next to SI-3a (Geyer et al., 1996). Rathelot et al. (Rathelot & Strick, 2009) showed a differential distribution of the cortico-motoneuronal cells for MI-4a and MI-4p in the macaque brain, resulting in a new view of MI organization, with monosynaptic connections from MI-4a to interneurons in the intermediate zone of the spinal cord, and monosynaptic connections from MI-4p directly to motoneurons in the ventral horn of the spinal cord. Monosynaptic input from the cerebral cortex to motoneurons is a relatively new phylogenetic feature (Kuypers, 1981), providing the ability to produce independent movements of the fingers and thus skilled movements such as precise grasp and tool manipulation. As a result, MI-4p is considered as the new MI, as compared to the phylogenetically older MI-4a, which is associated with less complex motor patterns (Rathelot & Strick, 2009). In humans, the functional role of MI-4a and MI-4p in human studies remains debated. On one hand, an fMRI study in healthy participants has observed a functional dissociation between MI-4a and MI-4p, with higher fMRI activity related to a flexion-extension task of the fingers in MI-4a than in MI-4p, while the reverse was observed for a sequential finger tapping requiring to move the fingers independently (Jaillard, Martin, Garambois, Lebas, & Hommel, 2005). Similar dissociations were also found in other stroke studies. The anatomo-functional subdivision of MI hand area has been related to subregions subserving different roles in motor control with MI-4p recruited by tasks engaging cognitive (Sharma, Jones, Carpenter, & Baron, 2008), attentional (Binkofski et al., 2002) or distal components (Vigano et al., 2019). In contrast, a meta-analysis showed that MI-4a activity was related to precision (versus force) handgrip, and MI-4p was related to dynamic (versus static) handgrip (King, Rauch, Stein, & Brooks, 2014). Here, we explored MI-4a and MI-4p separately, based on the assumption that MI-4p may be the output of precise grip tasks requiring independent finger movements, while MI-4a would drive simple motor tasks without independent finger movements, such as handgrip.

The main goal of this study was to determine using fMRI the neural structures engaged in motor hand recovery, in relation with the dorsolateral and dorsolateral frontoparietal circuits and the dual visuomotor model.

We first characterized motor hand recovery in patients with moderate to severe ischemic hemispheric stroke with two types of grasping tasks: a handgrip force task measuring the maximum force grip using a dynamometer, and a reach and grasp task requiring manual dexterity (i.e. precision grip) using the Purdue pegboard Task (PPT). Second, we measured fMRI activity elicited by a passive sensorimotor task of the paretic hand as described in Hannanu et al. (2017). As the regional fMRI BOLD-contrast signal is monotonically related to underlying neural activity in the frontoparietal cortex, it is possible, by comparing movement and rest periods, to measure changes in sensorimotor system activity reflecting motor behavioral performances following stroke. Therefore, to assess the neural correlates of handgrip force and PPT, we correlated behavioral performances

with fMRI activity measures from the sensorimotor network including the dorsolateral and dorsomedial regions during stroke recovery. We used a passive sensorimotor task because most patients were not able to perform active hand movements due to upper limb motor paresis at the subacute period of stroke. During the passive task, an examiner standing in the scanner room during the fMRI scan performed the flexion extension of the patient's paretic wrist. As both motor behavioral performances and fMRI activity patterns change during motor recovery (Favre et al., 2014; Marshall et al., 2000), we performed a longitudinal study combining behavioral and fMRI measurements at one month following stroke (M0), and six months (M6) and 24 months (M24) later.

Third, to determine the neural structures engaged in recovery of handgrip force and PPT, we modeled handgrip and PPT recovery using linear mixed models (LMMs) testing the effects of fMRI activity of ROIs spanning the frontoparietal networks on motor recovery. We also tested the effects of stroke features in the LMMs, including the hemispheric side of the lesion due to frontoparietal pathway asymmetry (Sainburg, 2002; Thiebaut de Schotten et al., 2011). Of note, patients were enrolled in a clinical trial assessing stem cell therapy (Jaillard et al., 2020). They were included at one month following stroke (M0) and were followed until the late chronic period of stroke (M24).

2. Material and methods

We report how we determined our sample size, all data exclusions, all inclusion/exclusion criteria, whether inclusion/exclusion criteria were established prior to data analysis, all manipulations, and all measures in the study.

2.1. Participants

We performed the ISIS-HERMES study, a monocenter (Grenoble Alpes University Hospital (CHUGA), France), prospective, randomized, open-label, controlled trial with blind outcome evaluation. Patients were randomized to receive IV injection of MSCs (Treatment group) or rehabilitation alone (Control group). Both ISIS (Intravenous Stem cells after Ischemic Stroke) and HERMES (HEuristic value of multimodal MRI to assess MEsenchymal stem cell therapy in Stroke) studies were approved by the ethics committee (Comité de Protection des Personnes). The trial is registered with [ClinicalTrials.gov](https://clinicaltrials.gov), number NCT00875654.

We enrolled 31 patients aged 18–70 years with an ischemic stroke within the anterior circulation territory, less than two weeks post-onset, with persistent neurological deficits (NIHSS ≥ 7), assessed just before cell injection. We did not include patients with brainstem or minor stroke, previous neurological or psychiatric disease, or severe comorbid medical disease. All patients were admitted to the CHUGA Stroke Unit for inclusion and follow-up visits. They received standard medical and rehabilitation care. The baseline visit (M0) was performed just before the MSC injection. Follow-up visits were performed after six months (M6) and 24 months (M24) following M0.

Thirty two healthy participants aged 18–70 years were also included in the ISIS-HERMES study to undergo the experimental motor tasks and the MRI protocol.

All patients and healthy participants gave written informed consent.

2.2. Behavioral tests

Patients underwent the Purdue Pegboard Test [PPT] (<http://www.equipement-ergotherapie.com/8-dextérité-manipulation.html>) (Rapin, Tourk, & Costa, 1966) and the LaFayette Dynamometer (<https://www.prohealthcareproducts.com/100-kg-220lb-hand-grip-dynamometer-lafayette-instruments/>) (Sunderland, Tinson, Bradley, & Hewer, 1989) that were used as the main outcome measures at M0, M6, and M24.

The purpose of the PPT was to test fine manual dexterity comprising reaching and grasping components. Features of the measure are described online: https://www.strokengine.ca/en/indepth/ppt_indepth. During the test, patients were seated with the Purdue Pegboard on a table in front of him/her. The testing board consisted of a board with 2 cups across the top containing 25 pins each and two vertical rows of 25 small holes down the center. Patients were asked to place as many pins as possible down the row within 30 s, first with the paretic hand. We measured the total number of pins placed in the assigned row using the paretic hand in the allotted time. The trial was repeated 3 times and a PPT score was calculated based on the number of pins placed down averaged across the 3 trials. A score of 0 was given when the participant could not perform the task due to upper limb paresis.

The dynamometer by measuring grip force involves mainly grasping components. The purpose of the handgrip force test was to measure the maximum isometric force of the hand and forearm muscles. Patients held the dynamometer in the hand, with the arm at right angles and the elbow by the side of the body. They were asked to squeeze the dynamometer with maximum isometric effort, which is maintained for about 5 s, without other body movements (<https://www.topendsports.com/testing/tests/handgrip.htm>). The grip force score was obtained by computing the average of 3 trials. Both PPT and dynamometer provide reliable and valid evaluation for hand motor function (Heller et al., 1987), and force (Sunderland et al., 1989) respectively.

In addition, we assessed stroke severity using the National Institutes of Health Stroke Scale (NIHSS) (Brott et al., 1989), functional independence using the Barthel Index of activities of daily living (Mahoney & Barthel, 1965), and neurological disability using the Modified Rankin Score (mRS) (van Swieten, Koudstaal, Visser, Schouten, & van Gijn, 1988). Motor impairment was assessed with the motor-Fugl Meyer Score (FMS, range 0–100) (Sullivan et al., 2011). The motor-FMS is a validated and reliable scale assessing motor function based on reflex activity, volitional movements and coordination of the upper and lower limbs, widely used for post-stroke motor assessment in RCTs (Chollet et al., 2011).

Behavioral assessment was performed by a neuropsychologist (dynamometer, PPT), a stroke neurologist (neurological examination, NIHSS, Barthel, mRS) and a physiotherapist (FMS), all blind to treatment allocation, at baseline (one month after stroke) and at six and 24-month

follow-up. The behavioral and fMRI assessment time points are shown in Table 1.

2.3. MRI data acquisition

Passive task paradigm. We used a passive sensorimotor task for the paretic hand rather than an active task because most patients could not perform voluntary movements of the hand at baseline (M0), since they had hemiparesis due to stroke. Moreover, passive tasks have higher reproducibility because of lower associated neural activity variability related to the patient's degree of motor impairment, range, and speed of motion, and required effort. Test-retest reproducibility studies of passive limb movements have shown good reliability for both within and between sessions in healthy participants and stroke patients (Gountouna et al., 2010; Loubinoux et al., 2001; Quiton, Keaser, Zhuo, Gullapalli, & Greenspan, 2014). The task paradigm consisted of 8 cycles alternating 20 sec epochs of rest and 45° passive wrist flexion and extension at 1 Hz (Fig. 1). We studied the passive-FE for the paretic hand in patients and the right hand in healthy participants, as described in (Loubinoux et al., 2001) and (Hannanu et al., 2017). All participants were instructed to remain still and relaxed during the scan. One examiner standing inside the room administered movements by moving a forearm splint with an axis of rotation through the wrist. Movements were visually cued using a screen placed in front of the examiner. While care was taken to observe mirror movements of both hands and feet, none were observed.

MRI protocol. MRI was performed at 3T (Achieva 3.0T TX, Philips, The Netherlands) at the IRMaGe MRI facility (Grenoble, France) with a 32 channel head coil. We acquired high resolution structural images including sagittal 3D-T1-weighted (TR 7.75 ms, TE 3.62 ms, flip angle 9°, FOV: 252*192*252, 192 slices, voxel size = .98*0.98*1 mm, thickness = 1 mm, gap = 0 mm, duration = 339 sec) and 3D-FLAIR images (TR 8 sec, TE 342 ms, flip angle = 90°, FOV: 241*192*250, 274 slices, voxel size = .434*.434*.7 mm, thickness = 1.4 mm, gap = -.7 mm, duration = 424 sec). Then, we acquired 113 Echo planar images (EPI) for the passive task of the paretic hand using the following parameters: TR 3000 ms, TE 30 ms, field of view (FOV): 220*220*147 mm, 59 axial slices. Flip angle = 80°, voxels 2.3*2.3*2.3 mm³, gap = .25 mm, run duration = 348 s. Total acquisition time was 20 min. These sequences were part of the study MRI protocol including in the following order: T1, FLAIR, resting state, passive motor task, tactile sensory task, diffusion, and perfusion sequences. The total duration was one hour.

2.4. MRI data analysis

Lesion volumes were determined by manual delineation of FLAIR images (Kuhn et al., 1989) using MRIcron (<https://www.nitrc.org/projects/mricron>).

Data preprocessing and processing, was performed using Statistical Parametric Mapping (SPM12: <http://www.fil.ion.ucl.ac.uk/spm>), as described in (Hannanu et al., 2017). Of note, T1, FLAIR, and EPI images were not flipped. Following visual inspection for spatial artifacts, EPI time series were checked for temporal artifacts and realigned. Next, the T1-weighted and FLAIR images were coregistered and aligned to the mean of the EPI time series. Segmentation of the structural images (T1 and FLAIR) resulted in a deformation field that was used to spatially normalize the EPI data to Montreal Neurological Institute (MNI) space. Finally, the EPI images in MNI space were smoothed using a full-width at half maximum (FWHM) Gaussian kernel of 5*5*5 mm³. The structural T1-weighted and FLAIR images were also normalized to MNI space at 1 mm³ resolution. Intensity outliers were detected using ART (https://www.nitrc.org/projects/artifact_detect), with an interscan movement threshold of 1 mm, and a global interscan signal intensity threshold of 3 SD relative to the session mean. In 6 patients with significant head motions, the movement thresholds were adjusted to limit the number of outliers to 20% of the total volumes.

The first level voxel-wise analysis was performed in SPM12 using a general linear model including passive movement conditions, outliers and head motion estimates as regressors, and a high-pass (128hz) filter. The task regressors were convolved with a canonical HRF. Contrasts of the movement related parameter estimates were generated for subsequent ROI analyses.

To explore the relationship between the sensorimotor network and outcome, we selected a priori ROIs that are reported as part of the sensorimotor network, and the parietal areas of the dorsolateral and dorsomedial networks, resulting in 36 left and 36 right ROIs listed in Table 2. For more information on these ROIs, see (Borra et al., 2017; Doyon, Penhune, & Ungerleider, 2003; Eickhoff et al., 2010; Hannanu et al., 2017; Pandya, 2015b). Prefrontal, occipital and temporal areas were not included because they were not activated by the passive sensorimotor task (Fig. 2), and thus could not be sensitive to task effects. The 36*2 ROIs were extracted from the SPM Anatomy Toolbox (Eickhoff, Paus, et al., 2007) and from the AAL atlas (Tzourio-Mazoyer et al., 2002). Using these ROIs, we

Table 1 – Hand motor task including Purdue Pegboard Test (PPT) and Grip Force (Grip) and fMRI assessment time points.

Study time points	Mean Delay from stroke onset	Hand motor tasks	MRI	Clinical assessment
Stroke onset	Day 0	–	–	NIHSS
Inclusion	Day 4–15	–	–	NIHSS + MRS + BI
Baseline visit (M0)	Day 31 (27–35)	PPT + Grip	fMRI	NIHSS + MRS + BI
Cell therapy	Day 32 (28–35)	–	–	NIHSS
Six-month follow-up (M6)	Day 210 (±15)	PPT + Grip	fMRI	NIHSS + MRS + BI
Two-year follow-up (M24)	Day 760 (±30)	PPT + Grip	fMRI	NIHSS + MRS + BI

NIHSS indicates the National Institutes of Health Stroke Scale, mRS the modified Rankin Score, and BI the Barthel Index.

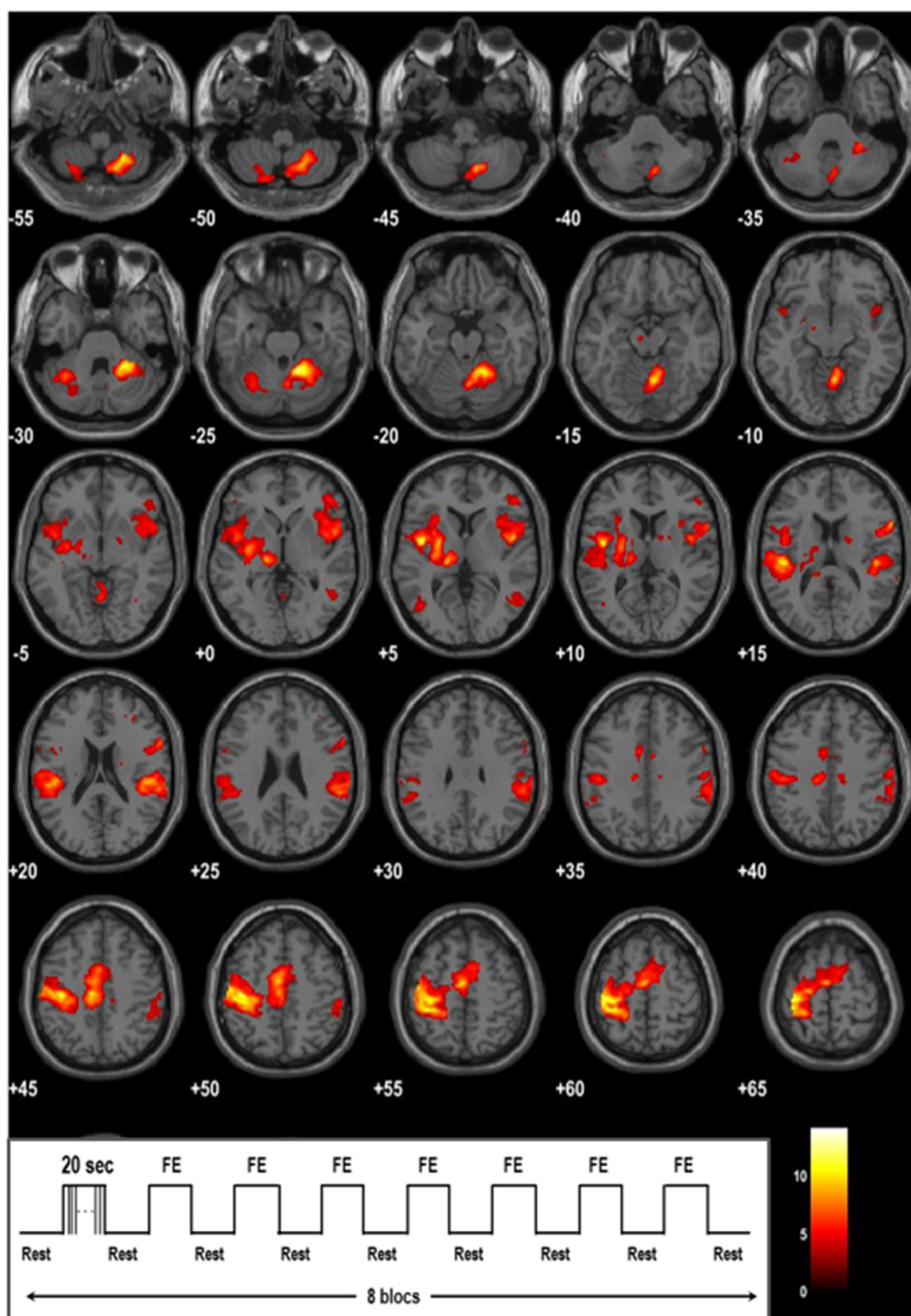


Fig. 1 – T1-rendered montage of brain activity during passive movement of the right hand in 32 healthy participants. Axial slices are displayed with for z MNI coordinates indicated in the bottom left corner in mm. A threshold of $p < .05$ corrected for multiple comparisons is used to allow visualization of the spatial distribution of activity. The color of the bar indicates the intensity of brain activity (t-statistic). The right hand is the referent hand. The left hemisphere is represented on the left side of picture (neurological convention).

Table 2 – Abbreviations for the 36 brain regions included in the analysis. In the text, i-indicates ipsilesional and c-contralesional ROIs. BA indicates Brodmann area and IPL inferior parietal lobule.

No.	Abbreviation	Full ROI Name
1.	MI-4a	Primary Motor cortex (MI) BA 4a
2.	MI-4p	Primary Motor cortex (MI) BA 4p
3.	SI-3a	Primary Somatosensory cortex (SI) BA 3a
4.	SI-3b	Primary Somatosensory cortex (SI) BA 3b
5.	SI-1	Primary Somatosensory cortex (SI) BA 1
6.	SI-2	Primary Somatosensory cortex (SI) BA 2
7.	dPMC	dorsal PreMotor Cortex BA6
8.	vPMC	ventral PreMotor Cortex BA6
9.	SMA	Supplementary Motor Area BA6
10.	Cereb V	Cerebellum lobule V
11.	Cereb VI	Cerebellum lobule VI
12.	Cereb VIIIa	Cerebellum lobule VIIIa
13.	Cereb VIIIb	Cerebellum lobule VIIIb
14.	MCA	Motor Cingulate Area
15.	BA44	BA44
16.	Insula	Anterior Insula
17.	Lenticular	Lenticular nucleus
18.	Thal-M	Motor Thalamus
19.	Thal-M	Somatosensory Thalamus
20.	OP1	Parietal operculum OP1 (S2)
21.	OP4	Parietal operculum OP4 (PV)
22.	IPL PF	Inferior Parietal Lobule (IPL) Supramarginal gyrus (SMG) BA 40 F
23.	IPL PFCm	IPL SMG BA 40
24.	IPL PFM	IPL SMG BA 40
25.	IPL PFop	IPL SMG BA 40
26.	IPL PFT	IPL SMG BA 40
27.	AIPS IPL1	Ventral anterior intraparietal sulcus (vAIPS) hIP1 (Scheperjans 2008a, b)
28.	AIPS IPL2	Lateral anterior intraparietal sulcus (lAIPS) hIP2 (Choi 2006)
29.	AIPS IPL3	Anterior medial intraparietal sulcus (amIPS) (Scheperjans 2008a, b)
30.	SPL 5ci	Superior Parietal Lobule (SPL) BA 5ci
31.	SPL 5L	SPL BA 5L
32.	SPL 5M	SPL BA 5M
33.	SPL 7A	Superior Parietal Lobule (SPL) BA 7A
34.	SPL 7M	SPL BA 7M (Posterior precuneus, hypothetic V6Ad)
35.	SPL 7P	SPL BA 7P
36.	SPL 7 PC	SPL BA 7 PC

computed peak ROI Cohen's *d* effect sizes (*d* values) that were derived from *t* maps for each participant using the 'Volumes toolbox' SPM extension (Volkmar Glaucher <http://sourceforge.net/projects/spmtools>). Cohen's *d* values were used to assess the relationship between passive-FE related brain activity and behavioral scores.

2.5. Statistical analysis

Clinical characteristics and behavioral scores are reported using: 1) median with percentiles and mean with standard deviations for continuous data and 2) absolute counts and percentages for categorical data. PPT and handgrip tests were scored 0 when patients could not perform the tasks due to hand paresis. Comparisons of PPT and handgrip performances between healthy participants and patients at each session were performed using univariate analyses of variance (ANOVA) after adjusting for the effects of age and sex and bootstrapping with 1000 replications. The influence of time and sensorimotor activity on hand motor recovery was analyzed using a linear mixed model (LMM)

accommodating repeated measures and including patient as a random effect (Cheng, Edwards, Maldonado-Molina, Komro, & Muller, 2010; Maas & Snijders, 2003). The dependent variables were the behavioral scores measured 3 times per patient. For both PPT and grip force scores, we first modeled the fixed effects of time from M0 (baseline), M6, and M24 (end of follow-up), adjusting for cell therapy and lesion side. Bonferroni correction was applied for adjustment for multiple comparisons of sessions. Then, we tested the effects of sensorimotor activity on PPT and handgrip over time, after adjustment for cell therapy. The effects of demographic and stroke characteristics including age, sex, lesion side, and volume were also tested and kept in the model if significant. Statistical significance was determined with the *F*-test ($p < .05$) and model fit was estimated with the $-2 \log$ likelihood ($-2LL$), Akaike Information Criterion (AIC), calibration and discrimination (Steyerberg et al., 2001). Calibration was examined by plotting adjusted predicted versus observed values for the behavioral scores. Discrimination assessed prediction accuracy by examining the distribution of the Pearson residuals and plotting residuals

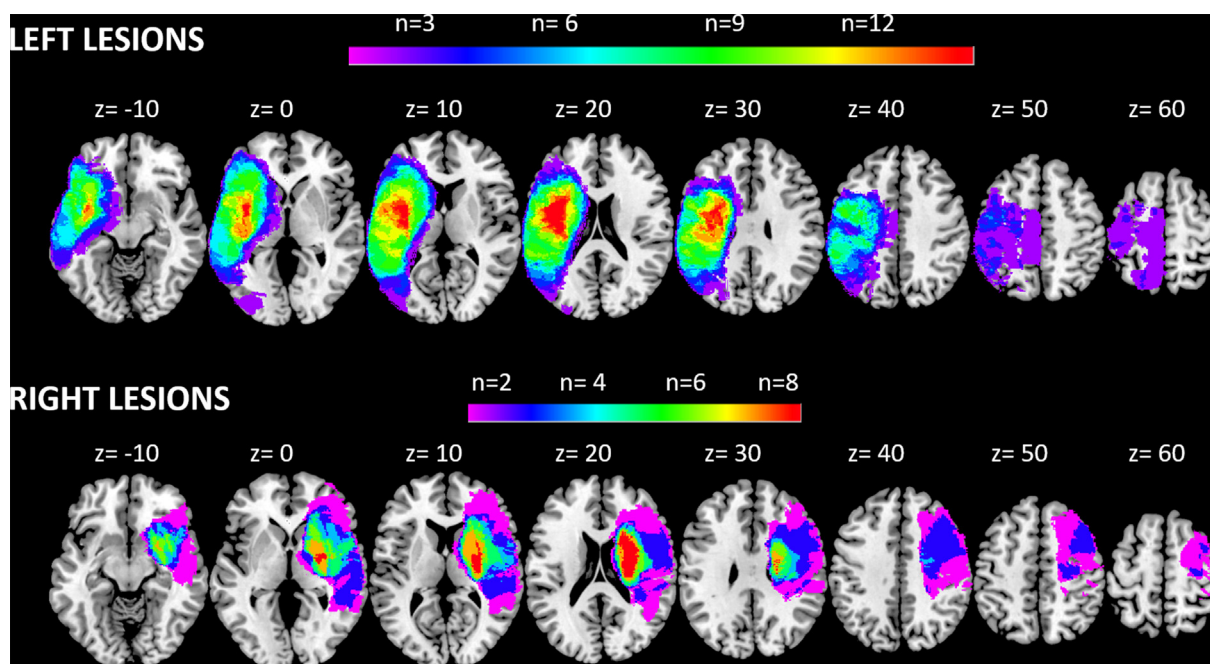


Fig. 2 – Overlay lesion plots of the 27 patients with left and right hemispheric stroke lesions. The number of overlapping lesions (n) is shown by different colors coding increasing frequencies from violet to red.

versus observed values. SPSS 20.0 was used for data analysis.

3. Results

3.1. Participants

Thirty-one patients (mean age = 52 ± 10 years; 22 males; 21 left-sided) were recruited between Aug 31, 2010 and Aug 31, 2015. Five patients could not undergo hand motor evaluation because of stroke severity resulting in severe neglect ($N = 1$), anosognosia ($N = 1$), head movements ($N=1$), or refusal ($N = 1$).

Therefore, twenty-seven patients remained in the study (mean age = 52.69 ± 10 years; 19 males; 17 left-sided lesions). Mean baseline NIHSS = 13.74 ± 4.63 , and motor-FMS $36.41 = \pm 28.21$, indicating moderate to severe neurological deficits. Among the 27 patients, 13 received intravenous stem cell therapy at baseline (Jaillard et al., 2020). Patient characteristics at baseline are presented in Table 3. The left and right hemispheric overlapping lesions plots are presented in Fig. 2. In addition, Thirty two healthy participants were included in the study and underwent both behavioral and fMRI assessment (mean age = 25 ± 6 years; 15 males).

Behavioral measures: Descriptive statistics are presented in Table 4 for the 32 healthy participants and 27 patients.

Table 3 – Patients' characteristics at baseline (one month following stroke onset) for left and right lesion subgroup. N = 27.

Variables	All (n = 27)		Left Lesion (n = 17)		Right Lesion (n = 10)		p values*
	Mean (SD)	Median (IQR)	Mean (SD)	Median (IQR)	Mean (SD)	Median (IQR)	
Age, years	53.15 (9.54)	53 (13)	55 (8.79)	57 (16)	50 (10.40)	51 (13)	.204
Lesion volume, cm ³	100.67 (63.51)	83 (103)	105.65 (55.23)	112 (83)	92.20 (78.13)	57.50 (143)	.41
Motor FMS	36.41 (28.21)	31 (34)	43.53 (32.88)	34 (62)	24.30 (10.90)	20.50 (10)	.188
Motor NIHSS	6.38 (2.64)	6.50 (4)	6.19 (3.23)	6 (5)	6.70 (1.33)	7 (1)	.787
NIHSS	13.74 (4.63)	12 (5)	14.88 (5.46)	12 (10)	11.80 (1.48)	12 (2)	.376
Barthel Index	45 (31.89)	45 (55)	42.06 (35.97)	45 (63)	50 (24.38)	47.50 (31)	.606
Rankin	3.78 (.51)	4 (0)	3.71 (.59)	4 (1)	3.90 (.32)	4 (0)	.572
PPT - Paretic Hand	1.3 (3.28)	0 (0)	2.06 (3.98)	0 (3)	0 (0)	0 (0)	.24
Grip - Paretic Hand	3.93 (9.95)	0 (0)	6.24 (12.06)	0 (8)	0 (0)	0 (0)	.127
Categorical	n	%	n	%	n	%	
Male	19	70.4	11	64.7	8	80	.666
Cell therapy	13	48.1	9	52.9	4	40	.695

SD, standard deviation; IQR, interquartile range; FMS, Fugl–Meyer Scale; NIHSS, National Institutes of Health Stroke Scale. *Comparison of left and right lesion subgroup, Mann–Whitney U test was used for numerical variables, and Chi-square/Fisher test for categorical variables, comparing data from left and right side lesion subgroups.

Table 4 – Descriptive statistics (Mean, Standard Deviation (SD), Median, Interquartile Range (IQR)) for Purdue Pegboard Test (PPT) and grip force (Grip) performed with the dominant hand in 32 controls and the paretic hand in 27 patients assessed at baseline (M0), six month (M6) and two-year (M24) follow-up.

Group/Session		Performance	Mean	SD	Median	IQR
Healthy Participants (n = 32)		PPT	16.75	1.64	16.67	2.67
		Grip	30.44	11.77	26.585	14.92
Patients	M0 (n = 27)	PPT	1.3	3.279	0	0
		Grip	3.93	9.95	0	0
	M6 (n = 25)	PPT	2.84	4.58	0	7
		Grip	7	11.712	0	11
	M24 (n = 25)	PPT	3.48	5.144	0	9
		Grip	9.62	14.688	0	21

Stroke patients had significantly lower scores than healthy participants at each session in the PPT ($p = .001$) and handgrip ($p = .001$). There was no significant effect of age for PPT ($p = .852$) and handgrip ($p = .733$). In patients with stroke, men performed significantly better than women in the handgrip force ($p = .002$), but not in the PPT ($p = .125$). LMM analyses showed that PPT and grip force improved significantly over time, after adjusting for lesion side, and cell therapy, indicating significant recovery of hand motor function over time (Table 5; Fig. 3). For PPT, there was a significant effect of time from baseline to M24 (mean difference = 1.65, $p = .010$) and from baseline to M6 (mean difference = 1.42, $p = .029$), but not between M6 and M24 (mean difference = .23, $p = 1.00$), with a significant effect of lesion side (mean difference 'left – right lesion' = 3.14, $p = .038$). For handgrip force, there was a significant effect of time from baseline to M24 (mean difference = 5.16, $p < .001$), with a trend from baseline to M6 (mean difference = 2.68, $p = .072$) and no difference between M6 and M24 (mean difference = 2.47, $p = .127$). There was a trend for the lesion side (mean difference 'left – right lesion' = 7.53, $p = .092$). Of note, age, gender, and lesion volume had no significant effect on recovery in these models.

3.2. MRI measures

The fMRI activity map related to the passive flexion extension (FE) of the right wrist in 32 healthy participants showed a typical activity in the sensorimotor network, and in posterior parietal areas (Fig. 1). To explore hand motor recovery using fMRI, we analyzed fMRI sessions in the 27 patients. Among the 81 scheduled sessions (3 time points for 27 patients), 13 fMRI sessions were not performed because of wrist spasticity and three additional sessions were excluded from analysis because

Table 5 – Linear mixed model of PPT and grip force showing the effects of time over time (2 years follow-up), lesion side and cell therapy, with F test and p values.

Factors	PPT		Handgrip force	
	F	p value	F	p value
Intercept	7.56	.011	7.02	.014
Time	5.74	.006	9.78	<.001
Lesion side	4.83	.038	3.08	.092
Cell therapy	2.05	.165	1.14	.296

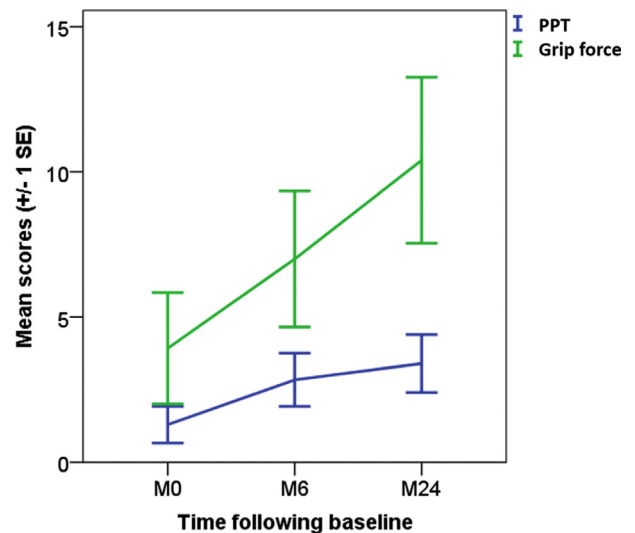


Fig. 3 – Performances of the Purdue Pegboard Test (PPT) and the handgrip force over time in 27 patients.

of excessive head movements (two sessions). The remaining 66 sessions (23 at M0, 25 at M6, and 18 at M24) were included for further analysis. Correlations between hand dexterity, grip force, and the sensorimotor regions are presented for each session (M0, M6 and M24) in Table 6 for the sensorimotor network and Table 7 for the posterior parietal cortex. Broadly, the correlations between most of the canonical motor ROIs and motor tasks were not significant at baseline (M0). Then, at M6, the ipsilesional canonical motor ROIs (except i-PMV), c-PMV, c-SMA, and contralesional cerebellar ROIs became significant. The other sensorimotor ROIs were not correlated with PPT and grip force at M0, except for c-MCA, c-BA44, and c-lenticular nucleus. In the posterior parietal network, IPL and OP ROIs at M0 were not correlated with PPT and grip force at M0, while the contralesional ROIs showed significant correlations with PPT and grip force at M6 and M24. By contrast, contralesional AIPs, and ipsilesional posterior/caudal SPL including BA 5M, 7A, 7M, and 7P showed significant correlations with motor tasks at M0 that faded over time. Of note, correlations were significant at M6 for ipsilesional BA 5L, 5M and 7A, and at M24 for ipsilesional BA 5L and 5M.

Hand motor recovery was explored using a LMM analysis including time and lesion side. Cell therapy was included in the model to account for any effect on the outcome. The best

Table 6 – Correlations between motor scores and fMRI activity in the sensorimotor network at M0, M6 and M24. *p* values are provided with bootstrapping (1000 replications). ROI correlations included in the LMM models are bold.

	M0				M6				M24			
	PPT		GRIP		PPT		GRIP		PPT		GRIP	
	<i>r</i>	<i>p</i>										
Canonical sensorimotor regions												
i-MI-4a	.332	.141	.294	.195	.552	.006	.606	.002	.653	.006	.597	.015
c-MI-4a	.295	.195	.341	.131	.646	.001	.599	.003	.333	.207	.598	.014
i-MI-4p	.327	.148	.411	.064	.444	.034	.452	.031	.508	.045	.439	.089
c-MI-4p	.208	.367	.366	.102	.217	.319	.185	.398	.273	.307	.287	.282
i-SI-3a	.406	.067	.441	.046	.532	.009	.464	.026	.718	.002	.454	.078
c-SI-3a	.247	.28	.377	.092	.342	.110	.176	.421	.232	.388	.256	.339
i-SI-3b	.297	.191	.294	.196	.537	.008	.570	.004	.569	.021	.514	.042
c-SI-3b	.29	.203	.38	.089	.629	.001	.507	.014	.238	.375	.384	.142
i-SI-1	.254	.266	.236	.303	.595	.003	.685	.000	.627	.009	.644	.007
c-SI-1	.381	.088	.412	.064	.615	.002	.485	.019	.227	.397	.379	.148
i-SI-2	.448	.042	.507	.019	.535	.008	.538	.008	.456	.088	.548	.034
c-SI-2	.416	.061	.474	.03	.593	.003	.495	.016	.13	.645	.24	.389
i-dPMC	.332	.141	.03	.187	.511	.013	.621	.002	.595	.015	.575	.02
c-dPMC	.253	.269	.241	.293	.486	.019	.452	.031	.188	.486	.29	.276
i-vPMC	-.069	.766	-.037	.873	.048	.829	-.034	.877	.135	.617	.022	.935
c-vPMC	.396	.075	.418	.06	.532	.009	.506	.014	.496	.051	.532	.034
i-SMA	.287	.207	.315	.164	.411	.052	.373	.080	.364	.166	.543	.03
c-SMA	.337	.135	.404	.069	.494	.017	.424	.044	.354	.178	.583	.018
Cerebellar network (cerebellar lobules)												
i-V	.035	.879	.07	.762	.284	.189	.217	.321	.573	.020	.464	.07
c-V	.217	.345	.105	.65	.643	.001	.544	.007	.771	.000	.610	.012
i-VI	-.12	.605	-.069	.767	.271	.211	.184	.400	.122	.653	.275	.303
c-VI	.338	.134	.428	.053	.63	.001	.492	.017	.779	.000	.583	.018
i-VIIIa	-.012	.96	-.046	.844	.309	.151	.185	.398	.385	.141	.413	.112
c-VIIIa	.275	.228	.27	.236	.495	.016	.312	.148	.579	.019	.444	.085
i-VIIIb	.066	.775	.169	.464	.403	.056	.216	.322	.31	.243	.349	.186
c-VIIIb	.402	.071	.372	.097	.47	.024	.275	.204	.612	.012	.399	.126
Sensorimotor related regions												
i-MCA	.147	.525	.268	.241	.351	.101	.308	.153	.229	.394	.376	.152
c-MCA	.294	.196	.449	.041	.361	.09	.208	.341	.295	.267	.325	.22
i-BA44	-.037	.875	-.06	.795	.002	.993	-.05	.822	.314	.237	.209	.437
c-BA44	.442	.045	.462	.035	.25	.25	.229	.294	.323	.222	.314	.236
i-ant Insula	.204	.376	.167	.469	-.07	.768	-.077	.727	.377	.149	.395	.13
c-ant Insula	.236	.302	.264	.247	.292	.177	.275	.205	.226	.399	.379	.148
i-lenticular	.088	.704	.002	.993	.201	.358	.009	.969	-.07	.804	.087	.748
c-lenticular	.411	.064	.454	.039	-.23	.301	-.262	.227	.03	.913	.114	.674
i-M-thal.	-.062	.789	-.171	.458	-.16	.461	-.161	.462	.085	.756	.128	.637
c-M-thal.	.222	.334	.261	.253	-.11	.625	-.227	.298	.004	.988	.123	.651
i-S-thal.	.095	.682	-.023	.921	-.17	.436	-.09	.682	.051	.85	.154	.568
c-S-thal.	.19	.41	.169	.463	.232	.287	.106	.632	.046	.866	.161	.552

r indicates Pearson's coefficient, i-for ipsilesional, and c-for contralesional. See Table 2 for the list of ROIs.

linear mixed model for dexterity recovery of the paretic hand assessed with PPT [-2LL = 255; AIC = 259; $R^2 = .93$] was obtained with a set of sensorimotor regions including ipsilesional MI-4p by time interaction [F (3, 33) = 3.82 $p = .019$], ipsilesional superior parietal lobule (SPL) 7M by time interaction [F (3, 31) = 4.79, $p = .007$], ipsilesional parietal operculum (OP1) [F (1, 39) = 9.1, $p = .004$], lesion side [F (1, 20) = 6.01, $p = .024$], and cell therapy [F (1, 22) = 1.32, $p = .26$]. Coefficient estimates are reported in Table 8. Significant ROIs are represented in Fig. 3A.

The LMM for grip force of the paretic hand [-2LL = 358; AIC = 362; $R^2 = .96$] included ipsilesional MI-4a by time interaction [F (1, 41) = 9.0, $p < .001$], ipsilesional OP1 [F (1,

42) = 7.32, $p = .011$], and contralesional IPL-PFt by lesion side [F (1, 37) = 8.95, $p = .001$], and cell therapy [F (1, 25) = .76, $p = .391$]. Coefficient estimates are reported in Table 9. Significant ROIs are represented in Fig. 4.

4. Discussion

This longitudinal study explored 27 patients with moderate to severe subacute stroke using concomitant sensorimotor hand behavioral and fMRI measurements with a passive FE task from the subacute to the chronic period of stroke. We assessed the relationship between manual dexterity and

Table 7 – Correlations between motor scores and fMRI activity in the posterior parietal cortex at M0, M6 and M24 (See Table 2 for ROI list). *p* values are provided with bootstrapping (1000 replications). ROI correlations included in the LMM models are bold.

	M0				M6				M24			
	PPT		GRIP		PPT		GRIP		PPT		GRIP	
	<i>r</i>	<i>p</i>										
Parietal operculum												
i- OP1	.122	.597	.181	.432	.527	.010	.590	.003	.454	.077	.534	.033
c-OP1	.068	.769	.096	.678	.593	.003	.599	.003	.334	.207	.483	.058
i-OP4	.148	.523	.134	.561	.331	.123	.194	.375	.449	.081	.318	.231
c-OP4	.394	.078	.327	.148	.574	.004	.604	.002	.317	.231	.522	.038
Inferior parietal lobule												
i-IPL-PF	.043	.854	.113	.626	.231	.288	.283	.191	.341	.196	.35	.184
c-IPL-PF	.346	.124	.349	.120	.641	.001	.543	.007	.571	.021	.616	.011
i-IPL-PFcm	.052	.822	.125	.589	.408	.054	.514	.012	.474	.064	.473	.064
c-IPL-PFcm	.173	.453	.171	.459	.463	.026	.309	.151	.339	.200	.411	.114
i-IPL-PFm	.055	.812	.015	.948	.262	.228	.288	.182	.168	.534	.276	.300
c-IPL-PFm	.297	.19	.41	.065	.481	.02	.355	.096	.478	.061	.572	.021
i-IPL-PFop	.097	.674	.19	.411	.418	.047	.576	.004	.381	.145	.472	.065
c-IPL-PFop	.147	.525	.15	.517	.677	.000	.634	.001	.512	.043	.642	.007
i-IPL-PFt	.021	.927	.063	.788	.184	.401	.13	.554	.191	.479	.261	.329
c-IPL-PFt	.306	.177	.342	.129	.738	.000	.645	.001	.549	.028	.634	.008
Anterior bank of intraparietal sulcus												
i-IPL-AIPS1	.221	.336	.139	.547	-.003	.99	.0740	.739	.642	.007	.553	.026
c-IPL-AIPS1	.432	.050	.553	.009	.226	.299	.193	.377	-.038	.89	.142	.599
i-IPL-AIPS2	.37	.098	.34	.132	.296	.170	.401	.058	.329	.213	.420	.105
c-IPL-AIPS2	.468	.032	.576	.006	.211	.333	-.008	.97	-.061	.824	-.022	.935
i-IPL-AIPS3	.414	.062	.355	.115	.183	.404	.118	.593	.210	.435	.24	.372
c-IPL-AIPS3	.515	.017	.571	.007	.257	.237	.235	.28	.147	.586	.188	.487
Superior parietal Lobule												
i-SPL-5ci	.028	.905	.095	.682	.197	.368	.11	.616	-.127	.64	.003	.991
c-SPL-5ci	.08	.73	.085	.714	.277	.201	.167	.447	.276	.301	.184	.496
i-SPL 5L	.216	.347	.224	.33	.63	.001	.649	.001	.592	.016	.656	.006
c- SPL 5L	.37	.099	.279	.221	.367	.085	.427	.042	.185	.494	.388	.137
i-SPL 5M	.516	.017	.634	.002	.477	.021	.418	.047	.428	.098	.633	.009
c- SPL 5M	.278	.223	.166	.472	.204	.35	.276	.203	-.005	.985	.136	.617
i-SPL 7A	.63	.002	.587	.005	.55	.007	.612	.002	.383	.143	.401	.124
c- SPL 7A	.278	.222	.232	.311	.068	.759	.036	.87	.064	.813	.081	.767
i-SPL 7M	.537	.012	.633	.002	.235	.280	.022	.919	.454	.077	.264	.322
c- SPL 7M	.415	.062	.481	.027	.197	.369	-.007	.975	.283	.289	.139	.607
i-SPL 7P	.509	.018	.452	.040	.219	.315	.022	.92	.151	.577	.044	.870
c- SPL 7P	.298	.190	.254	.266	.136	.535	.008	.971	-.043	.875	-.081	.766
i-SPL 7 PC	.310	.172	.351	.119	.348	.104	.237	.276	.268	.316	.351	.183
c- SPL 7 PC	.225	.328	.23	.315	.328	.126	.34	.113	.234	.383	.242	.367

r indicates Pearson's coefficient, i-for ipsilesional, and c-for contralesional. See Table 2 for the list of ROIs.

handgrip force and sensorimotor region activity at one month following stroke (M0) and then six months (M6) and two years later (M24). Then, using a linear mixed model analysis, we assessed the role of regional sensorimotor activity on hand motor recovery as a function of time. Our findings showed an association between fMRI activity patterns and hand motor recovery with a spatiotemporal pattern. Hand performance was correlated with fMRI activity in (1) AIPS and SPL ROIs at the early phase of recovery (M0); (2) bilateral regions of the sensorimotor network and the parietal operculum, IPL, and SPL at the early chronic phase of recovery (M6); (3) ipsilesional canonical areas and parietal regions (OP1, IPL, AIPS1 and SPL-5) at the late chronic phase of recovery (M24). These results are in line with the neuroimaging literature on stroke motor recovery supporting the idea that good recovery is associated with the restoration of a

normal activity pattern (Favre et al., 2014; Rehme et al., 2012). Furthermore, there was a dissociation between the recovery fMRI patterns of PPT and handgrip force. While PPT recovery was predicted by fMRI activity within i-MI-4p, and ROIs of both the dorsolateral network (i-OP1) and dorsomedial network (i-SPL-7M), handgrip force was predicted by activity in i-MI-4p, and ROIs of both the dorsolateral network including i-OP1 and c-IPL-PFt. These results suggest that the dual model based on segregated dorsolateral and dorsomedial streams can be applied to simple grasping tasks, but was challenged when considering in details the neural correlates of each task. We also found a dissociation between MI-4a related to handgrip force and MI-4p related to PPT, suggesting a functional specialization for these two MI areas as previously shown in the macaque (Rathelot & Strick, 2009). Finally, there was an effect of the lesion side, supporting

Table 8 – Estimates of fixed effect for the LMM of the PPT of the paretic hand.

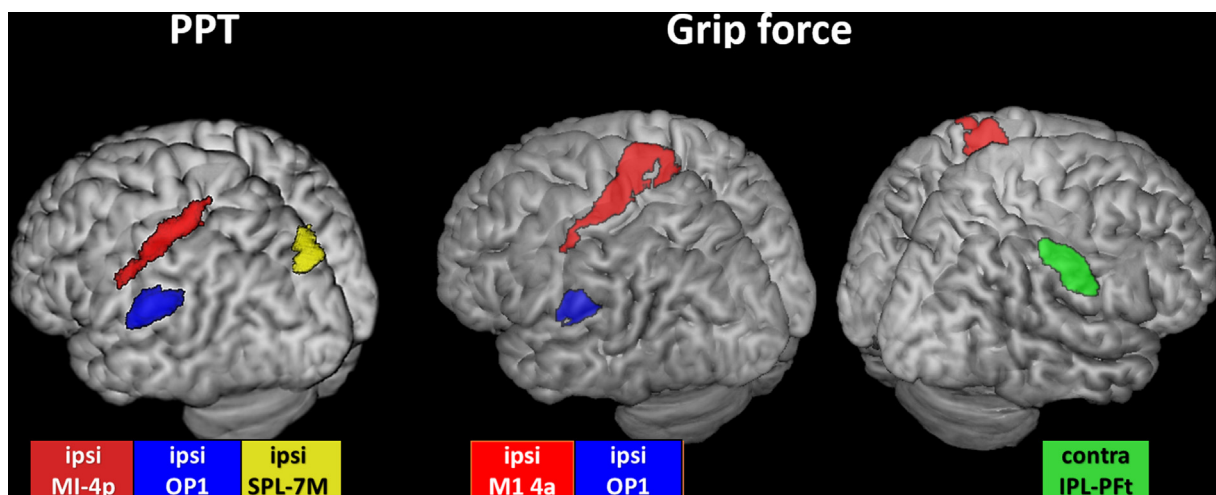
Parameter	Estimate	SE	df	t	p	95% CI	
						Lower	Upper
Intercept	.00	1.56	46.67	.00	.998	−3.13	3.13
Cell therapy (no/yes)	−1.69	1.47	22.27	−1.15	.262	−4.73	1.35
i-M1 4p by time							
i-M1 4p by M0	−2.90	1.12	36.57	−2.60	.013	−5.16	−.64
i-M1 4p by M6	−.12	.70	36.91	−.18	.861	−1.54	1.29
i-M1 4p by M24	.67	.82	34.44	.81	.423	−1.00	2.34
i-SPL 7M by time							
i-SPL 7M by M0	9.59	2.68	30.83	3.58	.001	4.13	15.05
i-SPL 7M by M6	3.74	1.49	32.37	2.51	.017	.71	6.78
i-SPL 7M by M24	2.01	1.65	30.18	1.22	.233	−1.36	5.37
i-OP1 (S2)	2.84	.94	38.58	3.02	.004	.94	4.75
Right lesion side	−3.57	1.46	19.72	−2.45	.024	−6.62	−.53

SE indicates standard error and CI indicates confidence interval.

Table 9 – Estimates of fixed effect for the LMM of the grip force of the paretic hand.

Parameter	Estimate	SE	df	t	p	95% CI	
						Lower	Upper
Intercept	6,86	3,72	42,29	1,84	0,072	−0,64	14,37
Cell therapy (no/yes)	−3,64	4,17	22,41	−0,87	0,391	−12,28	4,99
i-M1 4a by time							
i-M1 4a by M0	−3,00	1,30	32,73	−2,31	0,027	−5,64	−0,36
i-M1 4a by M6	−1,89	1,10	33,53	−1,72	0,094	−4,12	0,34
i-M1 4a by M24	0,46	1,07	32,82	0,43	0,668	−1,71	2,64
c-IPL -PFt by Lesion side							
c-IPL -PFt by Right lesion	−9,20	3,13	36,77	−2,94	0,006	−15,55	−2,85
c-IPL -PFt by Left lesion	4,06	2,41	38,55	1,68	0,100	−0,82	8,93
i-IPL OP1 (S2)	5,61	2,08	34,09	2,70	0,011	1,39	9,83

SE indicates standard error and CI confidence interval.

**Fig. 4 – Brain areas associated with Purdue Pegboard Test (PPT) and grip force recovery represented on 3D MNI brain template. Left indicates the left hemisphere.**

previous lines of evidence on brain asymmetries (Budisavljevic et al., 2017).

4.1. Recovery of hand motor function over time

In this longitudinal study, we observed significant improvement of hand motor performances over time (Table 4, Fig. 2). Indeed, the clinical LMMs modelling the repeated measures of PPT and handgrip showed a significant effect of time, confirming that the chronic stage is reached between six months and two-years following stroke onset (Kwakkel, Kollen, & Krakauer, 2014). In addition, the LMMs revealed lateralized lesion effects for the PPT with a trend for the handgrip force, such that patients with a right-sided lesion had worse recovery than those with a left-sided lesion. This finding is not explained by the lesion volume or stroke severity that were higher in patients with a left-sided lesion (Table 3). The prevalent view of brain organization posits right hemisphere specialization for spatial attentional and spatial cognitive processing (Mesulam, 1981; Thiebaut de Schotten et al., 2011). Therefore, cognitive deficits related to right hemispheric damage such as hemiasomatognosia and unilateral neglect may be responsible for an impairment of the body representation (Clark & Bindschlaeder, 2014). In line with this literature, our findings suggest that right hemispheric lesions might impair tasks requiring visuomotor transformations such as PPT, as the non-dominant right hemisphere is related to temporal aspects of movement and grasp pre-shaping (Budisavljevic et al., 2017). However, these interpretations are limited by the small sample size of this study.

4.2. Spatiotemporal pattern for the sensorimotor network

At baseline (M0), there were almost no significant correlations between hand motor performances and fMRI activity in the canonical sensorimotor network (Table 6). Indeed, few patients could perform the PPT and grip force tasks at baseline, and task performance remained very low over the two-year follow-up, reflecting the severity of stroke in our sample (Tables 3 and 4). Of note, there were significant correlations between handgrip and the somatosensory areas SI-3a and SI-2, as well between PPT and SI-2, underlining the role of these proprioceptive and tactile areas that provide somatosensory feedback to enable real-time adjustments of grasping (Gardner, Ro, Babu, & Ghosh, 2007) and encodes kinematics of the arm including hand trajectory through space during reaching movements (Chowdhury, Glaser, & Miller, 2020; London & Miller, 2013; Prud'homme & Kalaska, 1994). At six-month follow-up, we found positive correlations between hand motor performances and bilateral activity in the sensorimotor network, suggesting that the contralesional motor network may contribute to recovery until the early chronic phase of stroke. Then, at two-year follow-up, higher motor performances were correlated with activity in the ipsilesional sensorimotor network and parietal regions. Our results are in line with the literature based on meta-analyses of previous neuroimaging studies using active and passive motor tasks showing that brain activity during movements of the paretic hand follows a temporal pattern during stroke

recovery: during the early period of recovery, task-related fMRI cerebral activity is characterized by bilateral activity within the sensorimotor network, when compared with healthy participants, followed by the restoration of the physiological hemisphere activation balance (i.e. ipsilesional sensorimotor activity) at the chronic stage in patients with good functional recovery (Calautti et al., 2006; Carey, Abbott, Egan, Bernhardt, & Donnan, 2005; Rehme et al., 2015; Ward, 2005). Here, this temporal pattern was somewhat delayed to the early and late chronic period of recovery. This delay might be related to the motor impairment and stroke severity of this study that may have influenced hemispheric activation balance, as the contralesional MI may facilitate motor compensatory recovery in patients with severe motor impairment (Bradnam, Stinear, Barber, & Byblow, 2012).

4.3. Spatiotemporal pattern for the dorsolateral network

We found that hand motor performances for PPT and hand grip force were positively correlated with contralesional fMRI activity in the aIPS at the early period of recovery and in the IPL and OP1 at the chronic stages of stroke (Table 7). Furthermore, the LMM predicting handgrip force showed significant effects of the contralesional IPL-PfT (Table 9). These results are consistent with a previous fMRI stroke study, in which functional recovery of the upper limb was correlated with increased activity at the subacute stage of stroke in the ipsilesional rostral IPL (anterior supramarginal gyrus BA-40) (Loubinoux et al., 2003). Results from non-human primate studies have suggested that AIP, the putative nonhuman primate homolog of AIPS-IPL2 (Choi et al., 2006), is involved in grasping action and that PFG, the possible homolog of human IPL-PfT located in the rostral IPL (Caspers et al., 2011) participates in the process of action goals (Fogassi & Luppino, 2005). More recent works have confirmed these findings and identified both aIPS and PfT area/rostral IPL as key nodes of a network aimed at generating purposeful hand actions, recently referred as to the lateral grasping network (Borra et al., 2017). Functional MRI studies in healthy participants have suggested that aIPS was a key region of the dorsolateral circuit (Cavina-Pratesi et al., 2018), including manipulation of objects (Binkofski, Buccino, Posse, et al., 1999; Binkofski, Buccino, Stephan, et al., 1999), with a role in tactile exploration of objects and computation of visually guided grasping actions (Grefkes, Weiss, Zilles, & Fink, 2002; Tunik, Rice, Hamilton, & Grafton, 2007). Furthermore, we found a positive effect of the right PfT in patients with a left-sided lesion, and a negative effect of left IPL-PfT in patients with a right-sided lesion. Although there is some evidence that IPL is lateralized to the right to integrate visual and motor information for grasping execution (Fogassi & Luppino, 2005), others have reported a dominant arm advantage in controlling limb segment inertial interactions (Sainburg & Kalakanis, 2000), arguing for the dynamic-dominance hypothesis proposed by Sainburg (Sainburg, 2002).

Along these lines, we found significant correlations between the parietal opercular area OP1 and c-OP4 and motor performance at the chronic period of stroke recovery. Moreover, OP1 was a predictive factor of behavioral motor recovery

in the LMM analyses. Indeed, the parietal operculum SII, including the areas OP1 and OP4 that are the human homologues of the nonhuman primate areas SII and PV, respectively (Eickhoff, Grefkes, Zilles, & Fink, 2007) (Disbrow, Litinas, Recanzone, Padberg, & Krubitzer, 2003; Eickhoff et al., 2010), are activated in different grasping tasks in humans (Castiello, Bennett, Bonfiglioli, & Peppard, 2000) and in macaques (Nelissen et al., 2018). In humans, OP1 (also denoted S2) occupies the caudal part of the parietal operculum while OP4 is lying in its anterior part (Eickhoff et al., 2010). In the nonhuman primate, SII, the ventral part of the inferior parietal cortex first described by Woosley (Woosley, 1958), belongs to the dorsolateral network (Borra et al., 2017). SII responds during haptic shape perception, and is activated bilaterally under unilateral stimulus conditions, suggesting that neurons in the human OP may have bilateral receptive field and haptic shape perception (Disbrow et al., 2003). SII is densely connected to proprioceptive somatosensory area SI-3b and the area 7b (SPL-7P in humans) (Disbrow et al., 2003), and to the inferior parietal lobule, thalamus, MI, PMv, PMd and BA44, enhancing its integrative role for controlling hand actions (Pandya, 2015a; 2015b). Furthermore, neurons with attention and stimulus discrimination properties have been described in SII, suggesting that human OP1 may facilitate the incorporation of proprioceptive information in processes related to movement preparation and execution (Eickhoff et al., 2010), thus providing useful proprioceptive feedback on handgrip force. An fMRI study in healthy participants reported higher activity in the left OP1 for power grip than for precision grip performed with the right hand, in line with our findings showing higher estimates for handgrip force than PPT (Ehrsson et al., 2000). In both human and nonhuman primates, OP4/PV has strong connections with PMC and superior parietal cortex (BA-7) (Disbrow et al., 2003) and is engaged in sensorimotor integration, incorporating tactile and proprioceptive feedback on reach and grasp movements in both preparation and control processes (Eickhoff et al., 2010). In healthy participants, both OP1 and OP4 respond during active roughness and length discrimination, complex object manipulation (Binkofski, Buccino, Stephan, et al., 1999), and are consistently activated during grasping (Cavina-Pratesi et al., 2018), supporting the role played by the parietal operculum in the recovery of PPT and handgrip force following stroke.

4.4. Spatiotemporal pattern for the dorsomedial network

We found that ipsilesional SPL ROIs including 5M, 7A, 7M, and 7P were correlated with both PPT and handgrip at the early recovery period (M0). These correlations remained significant for BA5-M at the chronic period and for 7A at M6, but faded with time for the most caudal 7M and 7P ROIs. In the LMM, area 7M had significant effects on PPT performance with a time by ROI interaction term, indicating that these effects predominated in the first phase of stroke recovery. The role of SPL in PPT recovery is supported by previous anatomical and fMRI human studies. According to somatosensory or visual feedback that is required, reaching movements may activate rostral SPL (SPL-5) and/or caudal SPL (SPL-7) (Scheperjans, Eickhoff, et al., 2008; Scheperjans,

Grefkes, Palomero-Gallagher, Schleicher, & Zilles, 2005; Scheperjans, Hermann, et al., 2008) (Wenderoth, Toni, Bedeleem, Debaere, & Swinnen, 2006). In the macaque, motor goal actions also elicited neuronal activity in multiple areas of the posterior parietal cortex (Buneo, Batista, Jarvis, & Andersen, 2008; Tunik et al., 2007). In this study, SPL-7M was a significant predictor of early PPT recovery (from M0 to M6). Area SPL-7M is lying in the most ventrocaudal and medial part of BA7, ventrocaudally with respect to SPL-7P, extending into the anterior wall of the parieto-occipital sulcus (Scheperjans et al., 2008b). Interestingly, saccade-related activity has been shown in area 7M, also referred as the posterior precuneus in (Cavanna & Trimble, 2006). According to (Pitzalis et al., 2015), this medial posterior part of BA-7 (SPL-7M) may be the putative human homologue of V6Ad, the dorsal part of V6A (Gamberini, Galletti, Bosco, Breveglieri, & Fattori, 2011). V6A, a visuomotor area lying in the parietal wall of the SPOC, has been divided into two cytoarchitectonic subregions called V6Av and V6Ad (Luppino, Ben Hamed, Gamberini, Matelli, & Galletti, 2005). The dorsal V6A (V6Ad) is lying anteriorly and dorsally to the ventral V6A (V6Av). While both contain grasping neurons, V6Ad is characterized by a high number of arm-reaching neurons and few neurons with a retinotopic organization, while the reverse organization is seen in the retinotopic V6Av (Gamberini et al., 2011; Pitzalis et al., 2015). In contrast to V6Av that is located in BA19, corresponding to Oc4d of the Juelich anatomical atlas, V6Ad may overlap parts of area SPL-7M. In both nonhuman (Gamberini et al., 2011) and human primates (Cavina-Pratesi et al., 2010, 2018; Vesia & Crawford, 2012), an important role in the control of reach-to-grasp movements has been shown for V6A. Indeed, a TMS study showed that V6A may specify the handgrip parameters in the early motor plan of an upcoming reach to grasp action (Vesia et al., 2017), suggesting that V6Ad may play a role on the PPT task in analyzing the somatosensory information and in monitoring reach-to-grasp movements (Pitzalis et al., 2015).

4.5. MI-4a and MI-4p dissociation

As hypothesized, there was a dissociation between hand motor task recovery and MI regional activity. This dissociation was reflected on a functional level in such a way that PPT performance relates to area MI-4p control, while the handgrip force relates to the modulation of area MI-4a. Our findings are in line with the view that caudal area MI-4p, which is characterized by direct monosynaptic connections to motoneurons of the anterior horn of spinal cord in the macaque, may allow humans to produce independent movements of the fingers and thus highly skilled tasks, such as the PPT (Lawrence & Hopkins, 1976; Rathelot & Strick, 2009). In contrast, hand grip performance relies more on the phylogenetically older rostral MI-4a. Cortico-motoneuronal cells from MI-4a have only indirect connections to the spinal cord motoneurons through the intermediate interneurons of the spinal cord, limiting hand motor function to actions without independent finger movements (Rathelot & Strick, 2009). In this view, it is possible to propose that the final output MI of the dual visuomotor theory could be dissociated into two

anatomo-clinical subregions, MI-4a for reaching and hand grasp, and MI-4p for precise grasp requiring independent digit movements.

4.6. Methodological considerations

A first limitation of the present study was the small sample size that may have underpowered the statistical analysis. Moreover, as many patients suffered a severe stroke, more than 75% of them could not perform the PPT at baseline. Therefore, our results might have been biased by a floor effect and reflect more the ability to perform the task than the task performance itself. A second limitation relates to the fact that our study was part of a randomized clinical trial assessing the safety and feasibility of cell therapy. As the treatment was introduced in the model, we think that the cell therapy did not modify our results. However, due to these limitations, our findings need to be replicated in further studies.

Another limitation is related to fMRI that is not a direct measure brain activity during a task, since fMRI activity is based on neurovascular coupling generating BOLD signal. Here, we measured the contrast between BOLD signal during the passive motor task and rest, reflecting changes in neural activity in the sensorimotor regions. Nevertheless, motor task-related fMRI has been widely used in clinical applications (Mahdavi et al., 2015), and is recommended for use as a clinical biomarker of sensorimotor performance and recovery (Boyd et al., 2017; Savitz, Cramer, Wechsler, & Consortium, 2014).

A strength of this study relates to the longitudinal design of the study allowing for repeated measures of the behavioral and fMRI data in the context of a clinical trial with multimodal measures. Also, the small voxel size of the EPI fMRI images ($2.3 \times 2.4 \times 2.5 \text{ mm}^3$), resulting in smoothed normalized voxels of 125 mm^3 , allowed us to use the Juelich anatomical atlas, consisting of ROIs characterized by an accurate and reliable location but relative small volumes (1230 mm^3 for left BA-7M).

5. Conclusion

The present study explored the neural correlates of recovery of two standardized hand motor tasks in patients with moderate to severe stroke during a period of two years following stroke. Our findings showed that hand motor recovery was associated with a set of sensorimotor areas modulated by time from the subacute to the late chronic period of stroke, and task modality, in terms of movement component (reach and/or grasp) and dexterity. Thus, PPT requiring reaching movements and dexterity, i.e. independent finger movements, was associated with MI-4p along with dorsomedial and dorsolateral areas. In contrast, hand grip force recovery, requiring grasping without independent finger movements and no reach component, engaged the phylogenetically older MI-4a and dorsolateral parietal areas. While this view needs to be tested in further studies, our work may contribute to better understand visuomotor actions in patients with brain damage to develop tailored motor rehabilitation programs at the individual level.

Authorship contribution statement

F.H. was involved in MRI data analysis, statistical analysis, data interpretation and manuscript writing. I.G. was involved in MRI data analysis, statistical analysis, data interpretation and reviewed the manuscript. O.D. (ISIS PI) enrolled the patients and was involved in behavioral data acquisition and patient clinical follow-up. B.N. was involved in study design, behavioral data acquisition, data interpretation and manuscript reviewing. A.J. (HERMES PI) was involved in study design, data analysis, statistical analysis, data interpretation, MRI data acquisition, and manuscript writing.

ISIS-HERMES study group

M Barbieux, A. Chrispin, M. Cucherat, P. Davoine, H. Egelhofer, I Favre-Wiki, K. Garambois, P. Garnier, J. Gere, N. Gonnet, S. Grand, O. Heck, MJG Hommel, A.V. Jaillard, A. Krainik, L. Lamalle, J.F. Le Bas, S Marcel, S. Miguel, A. A. Paris, D. Perennou, P. Pernot, F. Renard, M.J. Richard, G. Rodier, A. Thuriot, I. Tropres, V. Vadot, J. Warnking, and TA Zeffiro.

Ethics statement

All patients gave written informed consent. Both “ISIS” (Intravenous Stem cells after Ischemic Stroke) RCT and “HERMES” (HEuristic value of multimodal MRI to assess MEsenchymal stem cell therapy in Stroke), its MRI satellite study, was approved by the local ethics committee (‘Comité de Protection des Personnes’).

Dataset statement

The datasets for this manuscript are not publicly available because ISIS HERMES is a randomized clinical trial assessing cell therapy. The main article reporting safety, feasibility and efficacy results of autologous mesenchymal stem cells is under publication. The data are the property of the University Hospital of Grenoble-Alpes (France) who is responsible for the confidentiality. The conditions of our ethics approval do not permit public archiving of the behavioral, clinical or MRI data supporting this study. Readers seeking access to anonymised data should contact the lead author assia.jaillard@univ-grenoble-alpes.fr. Access will be granted to named individuals in accordance with ethical procedures governing the reuse of sensitive data. Specifically, requestors must meet conditions to obtain the data including the completion of a formal data sharing agreement.

Open Practices

The study in this article earned a Preregistered badge for transparent practices. The trial is registered with Clinical-Trials.gov, number NCT00875654.

Funding

The trial was sponsored by the CHU Grenoble Alpes. This work was funded by the French Ministry of Health: PHRCI Grant numbers: ISIS-07PHR04 and HERMES-2007-A00853-50.

The funder had no role in study design, data acquisition or data analysis. The authors had full access to data and had final responsibility for publication.

ISIS RCT (ISIS-07PHR04) is registered on ClinicalTrials.gov: number NCT00875654: <https://clinicaltrials.gov/ct2/show/NCT00875654?term=ISIS+stroke+stem+cells&rank=1>.

The study procedures and analyses reported in this paper did not deviate from the registered protocol.

Declaration of Competing Interest

The authors declare no conflict of interest.

Acknowledgments

MRI data acquisition was performed on a platform of France Life Imaging network partly funded by the grant “ANR-11-INBS-0006”. Data monitoring was performed by the Clinical Investigation Center (CIC) INSERM UMS 002 CHU Grenoble Alpes. Data analysis was partly supported by RESSTORE project (www.resstore.eu) funded by the European Commission under the H2020 program (Grant Number 681044). Fabrice Hannanu PhD was funded by the Indonesia Endowment Fund for Education.

REFERENCES

- Berlot, E., Prichard, G., O'Reilly, J., Ejaz, N., & Diedrichsen, J. (2019). Ipsilateral finger representations in the sensorimotor cortex are driven by active movement processes, not passive sensory input. *Journal of Neurophysiology*, 121(2), 418–426. <https://doi.org/10.1152/jn.00439.2018>.
- Binkofski, F., Buccino, G., Posse, S., Seitz, R. J., Rizzolatti, G., & Freund, H. (1999). A fronto-parietal circuit for object manipulation in man: Evidence from an fMRI-study. *The European Journal of Neuroscience*, 11(9), 3276–3286.
- Binkofski, F., Buccino, G., Stephan, K. M., Rizzolatti, G., Seitz, R. J., & Freund, H. J. (1999). A parieto-premotor network for object manipulation: Evidence from neuroimaging. *Experimental Brain Research*, 128(1–2), 210–213.
- Binkofski, F., Fink, G. R., Geyer, S., Buccino, G., Gruber, O., Shah, N. J., ... Freund, H. J. (2002). Neural activity in human primary motor cortex areas 4a and 4p is modulated differentially by attention to action. *Journal of Neurophysiology*, 88(1), 514–519. <https://doi.org/10.1152/jn.2002.88.1.514>.
- Blatow, M., Reinhardt, J., Riffel, K., Nennig, E., Wengenroth, M., & Stippich, C. (2011). Clinical functional MRI of sensorimotor cortex using passive motor and sensory stimulation at 3 Tesla. *Journal of Magnetic Resonance Imaging: JMRI*, 34(2), 429–437. <https://doi.org/10.1002/jmri.22629>.
- Borra, E., Gerbella, M., Rozzi, S., & Luppino, G. (2017). The macaque lateral grasping network: A neural substrate for generating purposeful hand actions. *Neuroscience and Biobehavioral Reviews*, 75, 65–90. <https://doi.org/10.1016/j.neubiorev.2017.01.017>.
- Boyd, L. A., Hayward, K. S., Ward, N. S., Stinear, C. M., Rosso, C., Fisher, R. J., ... Cramer, S. C. (2017). Biomarkers of stroke recovery: Consensus-based core recommendations from the stroke recovery and rehabilitation roundtable. *Neurorehabilitation and Neural Repair*, 31(10–11), 864–876. <https://doi.org/10.1177/1545968317732680>.
- Bradnam, L. V., Stinear, C. M., Barber, P. A., & Byblow, W. D. (2012). Contralateral hemisphere control of the proximal paretic upper limb following stroke. *Cerebral Cortex*, 22(11), 2662–2671. <https://doi.org/10.1093/cercor/bhr344>.
- Brott, T., Adams, H. P., Olinger, C. P., Marler, J. R., Barsan, W. G., Biller, J., et al. (1989). Measurements of acute cerebral infarction: A clinical examination scale. *Stroke; a Journal of Cerebral Circulation*, 20(7), 864–870.
- Budisavljevic, S., Dell'Acqua, F., Zanatto, D., Begliomini, C., Miotto, D., Motta, R., et al. (2017). Asymmetry and structure of the fronto-parietal networks underlie visuomotor processing in humans. *Cerebral Cortex*, 27(2), 1532–1544. <https://doi.org/10.1093/cercor/bhv348>.
- Buneo, C. A., Batista, A. P., Jarvis, M. R., & Andersen, R. A. (2008). Time-invariant reference frames for parietal reach activity. *Experimental Brain Research*, 188(1), 77–89. <https://doi.org/10.1007/s00221-008-1340-x>.
- Calautti, C., Jones, P. S., Persaud, N., Guineestre, J. Y., Naccarato, M., Warburton, E. A., et al. (2006). Quantification of index tapping regularity after stroke with tri-axial accelerometry. *Brain Research Bulletin*, 70(1), 1–7. <https://doi.org/10.1016/j.brainresbull.2005.11.001>.
- Carey, L. M., Abbott, D. F., Egan, G. F., Bernhardt, J., & Donnan, G. A. (2005). Motor impairment and recovery in the upper limb after stroke: Behavioral and neuroanatomical correlates. *Stroke; a Journal of Cerebral Circulation*, 36(3), 625–629. <https://doi.org/10.1161/01.STR.0000155720.47711.83>.
- Caspers, S., Eickhoff, S. B., Rick, T., von Kapri, A., Kuhlén, T., Huang, R., ... Zilles, K. (2011). Probabilistic fibre tract analysis of cytoarchitectonically defined human inferior parietal lobule areas reveals similarities to macaques. *Neuroimage*, 58(2), 362–380. <https://doi.org/10.1016/j.neuroimage.2011.06.027>.
- Castiello, U., Bennett, K. M., Bonfiglioli, C., & Peppard, R. F. (2000). The reach-to-grasp movement in Parkinson's disease before and after dopaminergic medication. *Neuropsychologia*, 38(1), 46–59. [https://doi.org/10.1016/S0028-3932\(99\)00049-4](https://doi.org/10.1016/S0028-3932(99)00049-4).
- Cavanna, A. E., & Trimble, M. R. (2006). The precuneus: A review of its functional anatomy and behavioural correlates. *Brain: a Journal of Neurology*, 129(Pt 3), 564–583. <https://doi.org/10.1093/brain/awl004>.
- Cavina-Pratesi, C., Connolly, J. D., Monaco, S., Figley, T. D., Milner, A. D., Schenk, T., et al. (2018). Human neuroimaging reveals the subcomponents of grasping, reaching and pointing actions. *Cortex; a Journal Devoted to the Study of the Nervous System and Behavior*, 98, 128–148. <https://doi.org/10.1016/j.cortex.2017.05.018>.
- Cavina-Pratesi, C., Monaco, S., Fattori, P., Galletti, C., McAdam, T. D., Quinlan, D. J., ... Culham, J. C. (2010). Functional magnetic resonance imaging reveals the neural substrates of arm transport and grip formation in reach-to-grasp actions in humans. *The Journal of Neuroscience: the Official Journal of the Society for Neuroscience*, 30(31), 10306–10323. <https://doi.org/10.1523/JNEUROSCI.2023-10.2010>.
- Cheng, J., Edwards, L. J., Maldonado-Molina, M. M., Komro, K. A., & Muller, K. E. (2010). Real longitudinal data analysis for real people: Building a good enough mixed model. *Statistics in medicine*, 29(4), 504–520.
- Choi, H. J., Zilles, K., Mohlberg, H., Schleicher, A., Fink, G. R., Armstrong, E., et al. (2006). Cytoarchitectonic identification

- and probabilistic mapping of two distinct areas within the anterior ventral bank of the human intraparietal sulcus. *Journal of Comparative Neurology Comp Neurol*, 495(1), 53–69. <https://doi.org/10.1002/cne.20849>.
- Chollet, F., Tardy, J., Albucher, J. F., Thalamas, C., Berard, E., Lamy, C., ... Loubinoux, I. (2011). Fluoxetine for motor recovery after acute ischaemic stroke (FLAME): A randomised placebo-controlled trial. *Lancet Neurology*, 10(2), 123–130. [https://doi.org/10.1016/S1474-4422\(10\)70314-8](https://doi.org/10.1016/S1474-4422(10)70314-8).
- Chowdhury, R. H., Glaser, J. I., & Miller, L. E. (2020). Area 2 of primary somatosensory cortex encodes kinematics of the whole arm. *Elife*, 9. <https://doi.org/10.7554/eLife.48198>.
- Clark, A. S., & Bindschlaeder, C. (2014). Unilateral neglect and anosognosia. In M. E. Selzer, A. S. Clark, L. G. Cohen, G. Kwakkel, & R. H. Miller (Eds.), *Textbook of neural repair and rehabilitation* (2nd ed., Vol. II, pp. 463–477). Cambridge: Cambridge University Press.
- Cramer, S. C., Weisskoff, R. M., Schaechter, J. D., Nelles, G., Foley, M., Finklestein, S. P., et al. (2002). Motor cortex activation is related to force of squeezing. *Human Brain Mapping Brain Mapp*, 16(4), 197–205. <https://doi.org/10.1002/hbm.10040>.
- Culham, J. C., & Valyear, K. F. (2006). Human parietal cortex in action. *Current Opinion in Neurobiology*, 16(2), 205–212. <https://doi.org/10.1016/j.conb.2006.03.005>.
- Dai, T. H., Liu, J. Z., Sahgal, V., Brown, R. W., & Yue, G. H. (2001). Relationship between muscle output and functional MRI-measured brain activation. *Experimental Brain Research*, 140(3), 290–300. <https://doi.org/10.1007/s002210100815>.
- Davare, M., Andres, M., Clerget, E., Thonnard, J. L., & Olivier, E. (2007). Temporal dissociation between hand shaping and grip force scaling in the anterior intraparietal area. *The Journal of Neuroscience: the Official Journal of the Society for Neuroscience*, 27(15), 3974–3980. <https://doi.org/10.1523/JNEUROSCI.0426-07.2007>.
- Davare, M., Andres, M., Cosnard, G., Thonnard, J. L., & Olivier, E. (2006). Dissociating the role of ventral and dorsal premotor cortex in precision grasping. *The Journal of Neuroscience: the Official Journal of the Society for Neuroscience*, 26(8), 2260–2268. <https://doi.org/10.1523/JNEUROSCI.3386-05.2006>.
- Dettmers, C., Fink, G. R., Lemon, R. N., Stephan, K. M., Passingham, R. E., Silbersweig, D., ... Frackowiak, R. S. (1995). Relation between cerebral activity and force in the motor areas of the human brain. *Journal of Neurophysiology*, 74(2), 802–815. <https://doi.org/10.1152/jn.1995.74.2.802>.
- Disbrow, E., Litinas, E., Recanzone, G. H., Padberg, J., & Krubitzer, L. (2003). Cortical connections of the second somatosensory area and the parietal ventral area in macaque monkeys. *Journal of Comparative Neurology Comp Neurol*, 462(4), 382–399. <https://doi.org/10.1002/cne.10731>.
- Doyon, J., Penhune, V., & Ungerleider, L. G. (2003). Distinct contribution of the cortico-striatal and cortico-cerebellar systems to motor skill learning. *Neuropsychologia*, 41(3), 252–262.
- Ehrsson, H. H., Fagergren, A., Jonsson, T., Westling, G., Johansson, R. S., & Forssberg, H. (2000). Cortical activity in precision- versus power-grip tasks: An fMRI study. *Journal of Neurophysiology*, 83(1), 528–536. <https://doi.org/10.1152/jn.2000.83.1.528>.
- Eickhoff, S. B., Grefkes, C., Zilles, K., & Fink, G. R. (2007). The somatotopic organization of cytoarchitectonic areas on the human parietal operculum. *Cerebral Cortex*, 17(8), 1800–1811. <https://doi.org/10.1093/cercor/bhl090>.
- Eickhoff, S. B., Jbabdi, S., Caspers, S., Laird, A. R., Fox, P. T., Zilles, K., et al. (2010). Anatomical and functional connectivity of cytoarchitectonic areas within the human parietal operculum. *The Journal of Neuroscience: the Official Journal of the Society for Neuroscience*, 30(18), 6409–6421. <https://doi.org/10.1523/JNEUROSCI.5664-09.2010>.
- Eickhoff, S. B., Paus, T., Caspers, S., Grosbras, M. H., Evans, A. C., Zilles, K., et al. (2007). Assignment of functional activations to probabilistic cytoarchitectonic areas revisited. *Neuroimage*, 36(3), 511–521. <https://doi.org/10.1016/j.neuroimage.2007.03.060>.
- Estevez, N., Yu, N., Brugger, M., Villiger, M., Hepp-Reymond, M. C., Riener, R., et al. (2014). A reliability study on brain activation during active and passive arm movements supported by an MRI-compatible robot. *Brain Topography*, 27(6), 731–746. <https://doi.org/10.1007/s10548-014-0355-9>.
- Favre, I., Zeffiro, T. A., Detante, O., Krainik, A., Hommel, M., & Jaillard, A. (2014). Upper limb recovery after stroke is associated with ipsilesional primary motor cortical activity: A meta-analysis. *Stroke; a Journal of Cerebral Circulation*, 45(4), 1077–1083. <https://doi.org/10.1161/STROKEAHA.113.003168>.
- Filimon, F., Nelson, J. D., Hagler, D. J., & Sereno, M. I. (2007). Human cortical representations for reaching: Mirror neurons for execution, observation, and imagery. *Neuroimage*, 37(4), 1315–1328. <https://doi.org/10.1016/j.neuroimage.2007.06.008>.
- Filimon, F., Nelson, J. D., Huang, R. S., & Sereno, M. I. (2009). Multiple parietal reach regions in humans: Cortical representations for visual and proprioceptive feedback during on-line reaching. *The Journal of Neuroscience: the Official Journal of the Society for Neuroscience*, 29(9), 2961–2971. <https://doi.org/10.1523/JNEUROSCI.3211-08.2009>.
- Fogassi, L., & Luppino, G. (2005). Motor functions of the parietal lobe. *Current Opinion in Neurobiology*, 15(6), 626–631. <https://doi.org/10.1016/j.conb.2005.10.015>.
- Frey, S. H. (2008). Tool use, communicative gesture and cerebral asymmetries in the modern human brain. *Philosophical Transactions of the Royal Society of London B Biological Sciences* *Philos Trans R Soc Lond B Biol Sci*, 363(1499), 1951–1957. <https://doi.org/10.1098/rstb.2008.0008>.
- Gamberini, M., Galletti, C., Bosco, A., Breveglieri, R., & Fattori, P. (2011). Is the medial posterior parietal area V6a a single functional area? *The Journal of Neuroscience: the Official Journal of the Society for Neuroscience*, 31(13), 5145–5157. <https://doi.org/10.1523/JNEUROSCI.5489-10.2011>.
- Gardner, E. P., Ro, J. Y., Babu, K. S., & Ghosh, S. (2007). Neurophysiology of prehension. II. Response diversity in primary somatosensory (S-I) and motor (M-I) cortices. *Journal of Neurophysiology*, 97(2), 1656–1670. <https://doi.org/10.1152/jn.01031.2006>.
- Geyer, S., Ledberg, A., Schleicher, A., Kinomura, S., Schormann, T., Burgel, U., ... Roland, P. E. (1996). Two different areas within the primary motor cortex of man. *Nature*, 382(6594), 805–807. <https://doi.org/10.1038/382805a0>.
- Goodale, M. A., & Milner, A. D. (1992). Separate visual pathways for perception and action. *Trends in Neurosciences*, 15(1), 20–25. [https://doi.org/10.1016/0166-2236\(92\)90344-8](https://doi.org/10.1016/0166-2236(92)90344-8).
- Gountouna, V. E., Job, D. E., McIntosh, A. M., Moorhead, T. W., Lymer, G. K., Whalley, H. C., ... Lawrie, S. M. (2010). Functional Magnetic Resonance Imaging (fMRI) reproducibility and variance components across visits and scanning sites with a finger tapping task. *Neuroimage*, 49(1), 552–560. <https://doi.org/10.1016/j.neuroimage.2009.07.026>.
- Grafton, S. T. (2010). The cognitive neuroscience of prehension: Recent developments. *Experimental Brain Research*, 204(4), 475–491. <https://doi.org/10.1007/s00221-010-2315-2>.
- Grefkes, C., Weiss, P. H., Zilles, K., & Fink, G. R. (2002). Crossmodal processing of object features in human anterior intraparietal cortex: An fMRI study implies equivalencies between humans and monkeys. *Neuron*, 35(1), 173–184.
- Grol, M. J., Majdandzic, J., Stephan, K. E., Verhagen, L., Dijkerman, H. C., Bekkering, H., ... Toni, I. (2007). Parieto-frontal connectivity during visually guided grasping. *The Journal of Neuroscience: the Official Journal of the Society for*

- Neuroscience, 27(44), 11877–11887. <https://doi.org/10.1523/JNEUROSCI.3923-07.2007>.
- Hannanu, F. F., Zeffiro, T. A., Lamalle, L., Heck, O., Renard, F., Thuriot, A., ... Group, I.-H. S. (2017). Parietal operculum and motor cortex activities predict motor recovery in moderate to severe stroke. *Neuroimage Clinical*, 14, 518–529. <https://doi.org/10.1016/j.nicl.2017.01.023>.
- He, S. Q., Dum, R. P., & Strick, P. L. (1993). Topographic organization of corticospinal projections from the frontal lobe: Motor areas on the lateral surface of the hemisphere. *The Journal of Neuroscience: the Official Journal of the Society for Neuroscience*, 13(3), 952–980.
- Heller, A., Wade, D. T., Wood, V. A., Sunderland, A., Hewer, R. L., & Ward, E. (1987). Arm function after stroke: Measurement and recovery over the first three months. *Neurologia I Neurochirurgia Polska*, 50(6), 714–719.
- Horn, U., Grothe, M., & Lotze, M. (2016). MRI biomarkers for hand-motor outcome prediction and therapy monitoring following stroke. *Neural Plasticity*, 2016, 9265621. <https://doi.org/10.1155/2016/9265621>.
- Howells, H., Thiebaut de Schotten, M., Dell'Acqua, F., Beyh, A., Zappala, G., Leslie, A., ... Catani, M. (2018). Frontoparietal tracts linked to lateralized hand preference and manual specialization. *Cerebral Cortex*, 28(7), 2482–2494. <https://doi.org/10.1093/cercor/bhy040>.
- Jaillard, A., Hommel, M., Moisan, A., Zeffiro, T., Favre-Wiki, I., Barbieux-Guillot, M., & ISIS-HERMES. (2020). Autologous mesenchymal stem cells improve motor recovery in subacute ischemic stroke: a randomized clinical trial. *Translational Stroke Research*. In press.
- Jaillard, A., Martin, C. D., Garambois, K., Lebas, J. F., & Hommel, M. (2005). Vicarious function within the human primary motor cortex? A longitudinal fMRI stroke study. *Brain: a Journal of Neurology*, 128(Pt 5), 1122–1138. <https://doi.org/10.1093/brain/awh456>.
- Jeannerod, M., Arbib, M. A., Rizzolatti, G., & Sakata, H. (1995). Grasping objects: The cortical mechanisms of visuomotor transformation. *Trends in Neurosciences*, 18(7), 314–320.
- Karl, J. M., & Whishaw, I. Q. (2013). Different evolutionary origins for the reach and the grasp: An explanation for dual visuomotor channels in primate parietofrontal cortex. *Frontiers in Neurology*, 4, 208. <https://doi.org/10.3389/fneur.2013.00208>.
- Keisker, B., Hepp-Reymond, M. C., Blickenstorfer, A., Meyer, M., & Kollias, S. S. (2009). Differential force scaling of fine-graded power grip force in the sensorimotor network. *Human Brain Mapping*, 30(8), 2453–2465. <https://doi.org/10.1002/hbm.20676>.
- King, M., Rauch, H. G., Stein, D. J., & Brooks, S. J. (2014). The handyman's brain: A neuroimaging meta-analysis describing the similarities and differences between grip type and pattern in humans. *Neuroimage*, 102 Pt 2, 923–937. <https://doi.org/10.1016/j.neuroimage.2014.05.064>.
- Kuypers, H. G. H. M. (1981). Anatomy of the descending pathways. In J. M. Brookhart, & M. V.B. (Eds.), *The nervous system* (vol. II, pp. 628 (597-666)). Baltimore, USA: American Physiology Society.
- Kwakkel, G., Kollen, B., & Krakauer, J. W. (2014). Predicting activities after stroke. In M. E. Selzer, A. S. Clark, L. G. Cohen, G. Kwakkel, & R. H. Miller (Eds.), *Textbook of neural repair and rehabilitation* (2nd ed., Vol. II, pp. 585–600). Cambridge: Cambridge University Press.
- Lawrence, D. G., & Hopkins, D. A. (1976). The development of motor control in the rhesus monkey: Evidence concerning the role of corticomotoneuronal connections. *Brain: a Journal of Neurology*, 99(2), 235–254.
- London, B. M., & Miller, L. E. (2013). Responses of somatosensory area 2 neurons to actively and passively generated limb movements. *Journal of Neurophysiology*, 109(6), 1505–1513. <https://doi.org/10.1152/jn.00372.2012>.
- Lotze, M., Beutling, W., Loibl, M., Domin, M., Platz, T., Schminke, U., et al. (2012). Contralesional motor cortex activation depends on ipsilesional corticospinal tract integrity in well-recovered subcortical stroke patients. *Neurorehabilitation and Neural Repair*, 26(6), 594–603. <https://doi.org/10.1177/1545968311427706>.
- Loubinoux, I., Carel, C., Alary, F., Boulanouar, K., Viillard, G., Manelfe, C., ... Chollet, F. (2001). Within-session and between-session reproducibility of cerebral sensorimotor activation: A test-retest effect evidenced with functional magnetic resonance imaging. *Journal of Comparative Neurology Cereb Blood Flow Metab*, 21(5), 592–607. <https://doi.org/10.1097/00004647-200105000-00014>.
- Loubinoux, I., Carel, C., Pariente, J., Dechaumont, S., Albuher, J. F., Marque, P., ... Chollet, F. (2003). Correlation between cerebral reorganization and motor recovery after subcortical infarcts. *Neuroimage*, 20(4), 2166–2180.
- Loubinoux, I., Dechaumont-Palacin, S., Castel-Lacanal, E., De Boissezon, X., Marque, P., Pariente, J., ... Chollet, F. (2007). Prognostic value of fMRI in recovery of hand function in subcortical stroke patients. *Cerebral Cortex*, 17(12), 2980–2987. <https://doi.org/10.1093/cercor/bhm023>.
- Luppino, G., Ben Hamed, S., Gamberini, M., Matelli, M., & Galletti, C. (2005). Occipital (V6) and parietal (V6A) areas in the anterior wall of the parieto-occipital sulcus of the macaque: A cytoarchitectonic study. *The European Journal of Neuroscience*, 21(11), 3056–3076. <https://doi.org/10.1111/j.1460-9568.2005.04149.x>.
- Maas, C. J. M., & Snijders, T. A. B. (2003). The multilevel approach to repeated measures for complete and incomplete data. *Quality and Quantity*, 37(1), 71–89.
- Mahdavi, A., Azar, R., Shoar, M. H., Hooshmand, S., Mahdavi, A., & Kharrazi, H. H. (2015). Functional MRI in clinical practice: Assessment of language and motor for pre-surgical planning. *The Neuroradiology Journal*, 28(5), 468–473. <https://doi.org/10.1177/1971400915609343>.
- Mahoney, F. I., & Barthel, D. W. (1965). Functional evaluation: The Barthel index. *Maryland State Medical Journal*, 14, 61–65.
- Marshall, R. S., Perera, G. M., Lazar, R. M., Krakauer, J. W., Constantine, R. C., & DeLaPaz, R. L. (2000). Evolution of cortical activation during recovery from corticospinal tract infarction. *Stroke; a Journal of Cerebral Circulation*, 31(3), 656–661.
- Mesulam, M. M. (1981). A cortical network for directed attention and unilateral neglect. *Annals of Neurology*, 10(4), 309–325. <https://doi.org/10.1002/ana.410100402>.
- Milner, A. D., & Goodale, M. A. (2008). Two visual systems reviewed. *Neuropsychologia*, 46(3), 774–785. <https://doi.org/10.1016/j.neuropsychologia.2007.10.005>.
- Nelissen, K., Fiave, P. A., & Vanduffel, W. (2018). Decoding grasping movements from the parieto-frontal reaching circuit in the nonhuman primate. *Cerebral Cortex*, 28(4), 1245–1259. <https://doi.org/10.1093/cercor/bhx037>.
- Pandya, D. N. (2015). *Cerebral cortex: Architecture, connections, and the dual origin concept*. Oxford University Press (ISBN 10: 0195385152 ISBN 13: 9780195385151 ed.).
- Pandya, D. N. (2015b). Motor system. In D. Pandya, M. Petrides, & P. B. Cipolloni (Eds.), *Cerebral cortex: Architecture, connections, and the dual origin concept*. Oxford University Press (ISBN 10: 0195385152 ISBN 13: 9780195385151 ed., pp. 141-177).
- Pitzalis, S., Fattori, P., & Galletti, C. (2015). The human cortical areas V6 and V6A. *Visual Neuroscience*, 32, E007. <https://doi.org/10.1017/S0952523815000048>.
- Prud'homme, M. J., & Kalaska, J. F. (1994). Proprioceptive activity in primate primary somatosensory cortex during active arm reaching movements. *Journal of Neurophysiology*, 72(5), 2280–2301. <https://doi.org/10.1152/jn.1994.72.5.2280>.

- Quiton, R. L., Keaser, M. L., Zhuo, J., Gullapalli, R. P., & Greenspan, J. D. (2014). Intersession reliability of fMRI activation for heat pain and motor tasks. *Neuroimage Clin*, 5, 309–321. <https://doi.org/10.1016/j.nicl.2014.07.005>.
- Rapin, I., Tourk, L. M., & Costa, L. D. (1966). Evaluation of the Purdue Pegboard as a screening test for brain damage. *Developmental Medicine and Child Neurology*, 8(1), 45–54.
- Rathelot, J.-A., & Strick, P. L. (2009). Subdivisions of primary motor cortex based on cortico-motoneuronal cells. *Philosophical Transactions of the Royal Society of London B Biological Sciences*, 364(1324), 918–923. <https://doi.org/10.1098/rstb.2008.0210>.
- Rehme, A. K., Eickhoff, S. B., Rottschy, C., Fink, G. R., & Grefkes, C. (2012). Activation likelihood estimation meta-analysis of motor-related neural activity after stroke. *Neuroimage*, 59(3), 2771–2782. <https://doi.org/10.1016/j.neuroimage.2011.10.023>.
- Rehme, A. K., Volz, L. J., Feis, D. L., Eickhoff, S. B., Fink, G. R., & Grefkes, C. (2015). Individual prediction of chronic motor outcome in the acute post-stroke stage: Behavioral parameters versus functional imaging. *Human Brain Mapping*. <https://doi.org/10.1002/hbm.22936>.
- Richards, L. G., Stewart, K. C., Woodbury, M. L., Senesac, C., & Cauraugh, J. H. (2008). Movement-dependent stroke recovery: A systematic review and meta-analysis of TMS and fMRI evidence. *Neuropsychologia*, 46(1), 3–11. <https://doi.org/10.1016/j.neuropsychologia.2007.08.013>.
- Sainburg, R. L. (2002). Evidence for a dynamic-dominance hypothesis of handedness. *Experimental Brain Research*, 142(2), 241–258. <https://doi.org/10.1007/s00221-001-0913-8>.
- Sainburg, R. L., & Kalakanis, D. (2000). Differences in control of limb dynamics during dominant and nondominant arm reaching. *Journal of Neurophysiology*, 83(5), 2661–2675. <https://doi.org/10.1152/jn.2000.83.5.2661>.
- Savitz, S. I., Cramer, S. C., Wechsler, L., & Consortium, S. (2014). Stem cells as an emerging paradigm in stroke 3: Enhancing the development of clinical trials. *Stroke; a Journal of Cerebral Circulation*, 45(2), 634–639. <https://doi.org/10.1161/STROKEAHA.113.003379>.
- Scheperjans, F., Eickhoff, S. B., Homke, L., Mohlberg, H., Hermann, K., Amunts, K., et al. (2008). Probabilistic maps, morphometry, and variability of cytoarchitectonic areas in the human superior parietal cortex. *Cerebral Cortex*, 18(9), 2141–2157. <https://doi.org/10.1093/cercor/bhm241>.
- Scheperjans, F., Grefkes, C., Palomero-Gallagher, N., Schleicher, A., & Zilles, K. (2005). Subdivisions of human parietal area 5 revealed by quantitative receptor autoradiography: A parietal region between motor, somatosensory, and cingulate cortical areas. *Neuroimage*, 25(3), 975–992. <https://doi.org/10.1016/j.neuroimage.2004.12.017>.
- Scheperjans, F., Hermann, K., Eickhoff, S. B., Amunts, K., Schleicher, A., & Zilles, K. (2008). Observer-independent cytoarchitectonic mapping of the human superior parietal cortex. *Cerebral Cortex*, 18(4), 846–867. <https://doi.org/10.1093/cercor/bhm116>.
- Sharma, N., Jones, P. S., Carpenter, T. A., & Baron, J. C. (2008). Mapping the involvement of BA 4a and 4p during motor imagery. *Neuroimage*, 41(1), 92–99. <https://doi.org/10.1016/j.neuroimage.2008.02.009>.
- Steyerberg, E. W., Harrell, F. E., Jr., Borsboom, G. J., Eijkemans, M. J., Vergouwe, Y., & Habbema, J. D. (2001). Internal validation of predictive models: Efficiency of some procedures for logistic regression analysis. *Journal of Comparative Neurology Clin Epidemiol*, 54(8), 774–781.
- Sullivan, K. J., Tilson, J. K., Cen, S. Y., Rose, D. K., Hershberg, J., Correa, A., ... Duncan, P. W. (2011). Fugl-meyer assessment of sensorimotor function after stroke: Standardized training procedure for clinical practice and clinical trials. *Stroke; a Journal of Cerebral Circulation*, 42(2), 427–432. <https://doi.org/10.1161/STROKEAHA.110.592766>.
- Sunderland, A., Tinson, D., Bradley, L., & Hewer, R. L. (1989). Arm function after stroke. An evaluation of grip strength as a measure of recovery and a prognostic indicator. *Neurologia I Neurochirurgia Polska*, 52(11), 1267–1272.
- Thiebaut de Schotten, M., Dell'Acqua, F., Forkel, S. J., Simmons, A., Vergani, F., Murphy, D. G., et al. (2011). A lateralized brain network for visuospatial attention. *Nature Neuroscience*, 14(10), 1245–1246. <https://doi.org/10.1038/nn.2905>.
- Tunik, E., Rice, N. J., Hamilton, A., & Grafton, S. T. (2007). Beyond grasping: Representation of action in human anterior intraparietal sulcus. *Neuroimage*, 36(Suppl 2), T77–T86. <https://doi.org/10.1016/j.neuroimage.2007.03.026>.
- Tzourio-Mazoyer, N., Landeau, B., Papathanassiou, D., Crivello, F., Etard, O., Delcroix, N., ... Joliot, M. (2002). Automated anatomical labeling of activations in SPM using a macroscopic anatomical parcellation of the MNI MRI single-subject brain. *Neuroimage*, 15(1), 273–289. <https://doi.org/10.1006/nimg.2001.0978>.
- van Swieten, J. C., Koudstaal, P. J., Visser, M. C., Schouten, H. J., & van Gijn, J. (1988). Interobserver agreement for the assessment of handicap in stroke patients. *Stroke*, 19(5), 604–607. <https://doi.org/10.1161/01.str.19.5.604>.
- Vesia, M., Barnett-Cowan, M., Elahi, B., Jegatheeswaran, G., Isayama, R., Neva, J. L., ... Chen, R. (2017). Human dorsomedial parieto-motor circuit specifies grasp during the planning of goal-directed hand actions. *Cortex; a Journal Devoted To the Study of the Nervous System and Behavior*, 92, 175–186. <https://doi.org/10.1016/j.cortex.2017.04.007>.
- Vesia, M., & Crawford, J. D. (2012). Specialization of reach function in human posterior parietal cortex. *Experimental Brain Research*, 221(1), 1–18. <https://doi.org/10.1007/s00221-012-3158-9>.
- Vigano, L., Forna, L., Rossi, M., Howells, H., Leonetti, A., Puglisi, G., ... Cerri, G. (2019). Anatomic-functional characterisation of the human "hand-knob": A direct electrophysiological study. *Cortex; a Journal Devoted To the Study of the Nervous System and Behavior*, 113, 239–254. <https://doi.org/10.1016/j.cortex.2018.12.011>.
- Ward, N. S. (2005). Mechanisms underlying recovery of motor function after stroke. *Postgraduate Medical Journal*, 81(958), 510–514. <https://doi.org/10.1136/pgmj.2004.030809>.
- Weiller, C., Juptner, M., Fellows, S., Rijntjes, M., Leonhardt, G., Kiebel, S., ... Thilmann, A. F. (1996). Brain representation of active and passive movements. *Neuroimage*, 4(2), 105–110. <https://doi.org/10.1006/nimg.1996.0034>.
- Wenderoth, N., Toni, I., Bedeleem, S., Debaere, F., & Swinnen, S. P. (2006). Information processing in human parieto-frontal circuits during goal-directed bimanual movements. *Neuroimage*, 31(1), 264–278. <https://doi.org/10.1016/j.neuroimage.2005.11.033>.
- Woolsey, C. N. (1958). Organization of somatic sensory and motor areas of the cerebral cortex. In H. F. Harlow, & C. N. Woolsey (Eds.), *Biological and biochemical bases of behavior* (pp. 63–81). Madison: University of Wisconsin Press.